Sesterterpenes as Tubulin Tyrosine Ligase Inhibitors. First Insight of Structure−Activity Relationships and Discovery of New Lead

Fabrizio Dal Piaz,[†,§] Antonio Vassallo,[†,§] Laura Lepore,[†] Alessandra Tosco,[†] Ammar Bader,[‡] and Nunziatina De Tommasi*[,†]

Dipartimento di Scienze Farmaceutiche, Università di Salerno, Via Ponte Don Melillo, 84084 Fisciano (SA), Italy, and Faculty of Pharmacy, Al-Zaytoonah Private University of Jordan, P.O. Box 130, 11733 Amman, Jordan

Received December 23, 2008

Twenty-four new sesterterpenes, compounds **1**−**24**, were isolated from the aerial parts of *Salvia dominica*. Their structures were elucidated by 1D and 2D NMR experiments as well as ESIMS analysis and chemical methods. The evaluation of the biological activity of *Salvia dominica* sesterterpenes by means of a panel of chemical and biological approaches, including chemical proteomics, surface plasmon resonance (SPR) measurements, and biochemical assays were realized. Obtained results showed that 18 out of the 24 sesterterpene lactones isolated from *Salvia dominica* interact with tubulin−tyrosine ligase (TTL) an enzyme involved in the tyrosination cycle of the C-terminal of tubulin, and inhibit TTL activity in cancer cells. Besides, results of our studies provided an activity/structure relationship that can be used to design effective TTL inhibitors.

Salvia is a very important genus comprising about 900 species in the family Lamiaceae. Plants belonging to this genus show high diversity in their secondary metabolites[1,2] as well as in pharmacological effects. Several *Salvia* species are included in many pharmacopeias and are also used for alimentary and cosmetic purposes.[3,4] The main secondary metabolites constituents of *Salvia* species are poliphenols, flavonoids, and terpenoids.[5,6]

As a part of an ongoing research program aimed at the isolation, structural characterization, and pharmacological evaluation of bioactive secondary metabolites from plants, we started the phytochemical analysis of *Salvia dominica* L.

S. dominica L. is known in Jordan as "Maru", and its leaves are used in the Jordanian popular folk medicine for cold, stomach pain, and indigestion; in addition, *S. dominica* produces edible galls.[7,8]

Our studies led to the isolation of 24 sesterterpene lactones, whose structures were secured by means of spectroscopy as well as mass spectrometry analyses and chemical evidence.

The sestertepenes are a relatively small group of terpenoids, their sources are widespread, having been isolated from terrestrial fungi, lichens, high plants, insects, and various marine organisms. Sesterterpenes exhibit different biological activities such as anti-inflammatory, cytotoxic, antifeedant, and antimicrobial.[9] The structural characteristics and the biological activities of sesterterpenes made them attractive targets for both biomedical and synthetic purposes.[10] However, the precise biological function and specific binding partners of these bioactive compounds are frequently unknown, hence they can be defined as "orphan" molecules. Complementary technologies are required for the identification of the specific targets for these and other orphan natural compounds. We describe herein a strategy for the evaluation of biological activity of *Salvia* sesterterpenes by means of a panel of chemical and biological approaches, including chemical proteomics, surface plasmon resonance measurements, and biochemical assays.

Chemical proteomics using compound-immobilized columns is a promising and powerful strategy for drug discovery because the elucidation of drug−protein complexes is a direct approach if compared to indirect analyses, such as 2-dimensional electrophoresis or the use of DNA chips to monitor changes of protein/mRNA expression.[11] An analysis of the targets would contribute to predict unexpected side effects for more effective clinical applications and possibly to highlight potential lead compounds. In addition, identification of drug-interacting proteins may provide clues to the functions of these proteins for other projects.

Our results showed that 18 out of the 24 sesterterpene lactones isolated from *Salvia dominica* interact with tubulin tyrosine ligase (TTL[a]), an enzyme involved in the tyrosination cycle of the C-terminal of tubulin.[12,13] TTL has been demonstrated to play a key role in many physiological processes and to be essential for neuronal organization.[14] Moreover, misregulation of tyrosination/detyrosination cycle of tubulin, frequently observed during cancer progression, is associated with increased tumor aggressiveness.[15−17] Thus, TTL could be a target for developing novel therapeutic strategies against cancer because modulators of TTL, by restoring normal Tyr-tubulin, could impair tumor progression.[14,17] Our data demonstrated that *S. Dominica* sesterterpenes are able to bind efficiently and to inhibit in cell-based assay TTL protein. The results showed the existence of defined structure/activity relationships, suggesting the involvement of the side chain fragment of the sesterterpenes in TTL binding. These data could be used to design effective TTL inhibitors.

Results and Discussion

Isolation and Structural Elucidation of Sesterterpenes. The $CHCl_3$ and $CHCl_3$−MeOH (9:1) extracts of the aerial parts of

* To whom correspondence should be addressed. Phone: +39-089-969754. Fax: +39-089-969752. E-mail: detommasi@unisa.it.
† Dipartimento di Scienze Farmaceutiche, Università di Salerno.
‡ Al-Zaytoonah University of Jordan.
§ Equal contributing authors.

[a] Abbreviations: TTL, tubulin tyrosine ligase; HRMS, high resolution mass spectrometry; MTPA, methoxy(trifluoromethyl)phenylacetyl); SPR, surface plasmon resonance; HEK293, human epithelial kidney cells; J774.A1, murine monocyte/macrophagycells; MCF-7, human breast adenocarcinoma cells; MTT, 3-(4,5-dimethylthiazol-2-yl)-2,5-diphenyltetrazolium bromide; TCP, tubulin-specific carboxypeptidase.

10.1021/jm801637f CCC: $40.75
Published on Web 05/21/2009

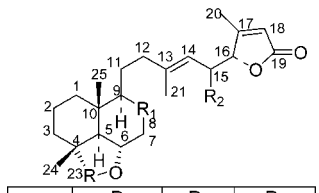

	R	R_1	R_2
1	$-CH_2$	=	-H
2	$-CH_2$	OH	-OH
3	-CO	OH	-OH
4	-CHOH	OH	-OH
5	-CHOEt	OH	-OH
6	-CHOEt	OH	-H

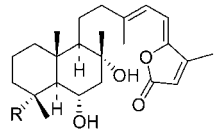

	R
17	$-CH_2OH$
18	-COOH
19	-CHO

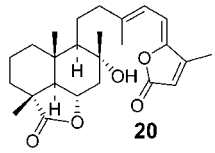

20

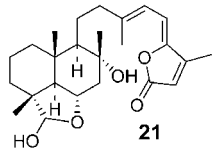

21

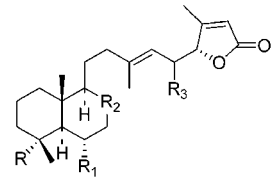

	R	R_1	R_2	R_3
7	$-CH_2OH$	-OH	OH	-OH
8	$-CH_2OH$	-OH	OH	-H
9	$-CH_3$	-OH	OH	-OH
10	-COOH	-OH	OH	-OH
11	-COOH	-OH	OH	-H
12	-COOMe	-OH	OH	-OH
13	-CHO	-OH	OH	-OH
14	-CHO	-OH	OH	-H
15	$-CH_2OH$	-OH	=	-OH
16	-CHO	-OH	=	-OH

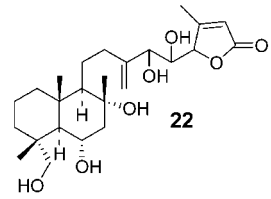

22

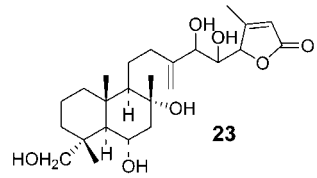

23

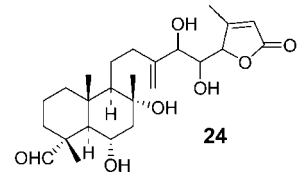

24

Figure 1. Compounds **1**−**24**.

Salvia dominica afforded 24 new sesterterpenes (**1**−**24**) (Figure 1), isolated by silica gel, Sephadex LH-20 column chromatography, and RP-HPLC.

The molecular formula of compound **1** $C_{25}H_{36}O_3$ was established by ^{13}C NMR and HRMS (obsd *m*/*z* 407.272 for $[M + Na]^+$ calcd *m*/*z* 407.256), indicating eight degrees of unsaturation.

An IR absorption band at 1780 cm^{-1} suggested the presence of an α,*β*-unsaturated lactone carbonyl functionality, which was supported by the presence of an ester carbonyl resonance at 175.0 ppm in the ^{13}C NMR spectrum.[18] The ^1H NMR spectrum showed the presence of a four methyls singlet at *δ* 2.12 (Me-20), 1.72 (Me-21), 1.11 (Me-24), 0.92 (Me-25), two oxymethines at *δ* 3.80 (H-6) and *δ* 5.07 (H-16), one oxymethylene at *δ* 3.62 and 3.44 (H_2-23), two trisubstituted olefinic protons at *δ* 5.05 (H-14) and *δ* 5.90 (H-18), and two disubstituted olefinic protons at *δ* 4.83 (H-22a) and *δ* 4.65 (H-22b). COSY and 1D-TOCSY measurement showing coupling between H-14−H_2-15-H-16, H-16−Me-20, and H-18−Me-20 established the spin system C-13−C-18. Proton resonance of H-18 at *δ* 5.90 showed a long-range COSY coupling to H-16. In addition, HMBC correlations from H-16 to C-18 (117.4 *δ*) confirmed the assignment of C-18. The carbonyl resonance at C-19 (175.0 *δ*) was assigned based of HMBC correlation from H-18 to C-19. A signal at *δ* 2.12 was consistent with the presence of a methyl group at C-17, and this was also supported by HMBC correlation of Me-20 and C-17; Me-20 also showed long-range COSY coupling to H-18, supporting the presence of an α,*β*-unsaturated butenolide moiety.[19] The linkage between C-15 and the butenolide group was deduced by HMBC correlations the H-15a signal at *δ* 2.38 correlated to *δ* 117.4 (C-18), *δ* 140.7 (C-13), *δ* 170.8 (C-17), and *δ* 5.07 (H-16) to C-18, C-19, C-14, and C-13. Results obtained from 1D-TOCSY and COSY experiments established the connectivity of proton H-9−H-11−H-12−H-14, confirmed by HMBC cross peaks between H-12 and C-9, C-14. The remaining part of molecule as inferred by the molecular formula and inspection of ^{13}C, and DEPT NMR spectra, had to be composed of 2 sp^2 hybridized carbon atoms and 11 sp^3 hybridized carbon atoms and must be tricyclic. 1D-TOCSY and COSY experiments provided evidence for the presence in the molecule of the segments H-1−H-3 and H-5−H-7. Furthermore, the HMBC correlations of H-6 signal centered

Table 1. NMR data of Compounds **1**−**2** (CD_3OD, 600 MHz)[a]

	1		**2**	
pos	δ_H	δ_C	δ_H	δ_C
1a	1.79[b]	41.7	1.80[b]	42.4
1b	1.06 (ddd, 13.0, 12.5, 4.0)		1.09 (ddd, 13., 12.5, 4)	
2a	1.36[b]	19.7	1.71[b]	19.7
2b	1.52[b]		1.36[b]	
3a	1.72 (m)	36.4	1.80[b]	36.4
3b	1.23 (m)		1.31[b]	
4		40.7		41.0
5	1.25 (d,10.0)	61.4	1.25 (d,10.5)	61.4
6	3.80 (ddd, 11.0, 10, 4.0)	73.6	3.79 (ddd, 11.0, 10, 4.8)	74.0
7a	2.39 (dd, 12.0, 4.8)	46.3	2.26 (dd, 12.0, 4.8)	46.5
7b	1.97 (dd, 13.0, 12.0)		1.48 (dd, 13.0, 12.0)	
8		149.0		76.0
9	2.00 (dd, 8.0, 5.5)	58.0	1.20 (dd, 6.0, 5.5)	62.0
10		37.5		37.3
11a	1.81[b]	23.7	1.68[b]	24.0
11b	1.38[b]		1.38 [b]	
12a	2.18 (ddd, 13.5,11.0, 3.5)	43.0	2.34 (ddd, 13.5,11.0, 3.5)	43.0
12b	2.02 (ddd, 13.5, 6.0, 3.5)		2.12 (ddd, 13.5, 6.0, 3.5)	
13		140.7		143.9
14	5.05 (dd, 8.0, 3.0)	116.5	5.29 (d, 8.8)	123.2
15a	2.74 (ddd, 13.5, 8.0, 5.5)	31.0	4.75 (dd, 8.8, 3.0)	67.0
15b	2.38 (ddd, 13.5, 6.0, 4.5)			
16	5.07 (m)	86.6	4.99 (d, 3.0)	88.7
17		170.8		170.7
18	5.90 (d, 1.3)	117.4	5.96 (d, 1.3)	118.6
19		175.0		174.0
20	2.12 (d, 1.3)	13.8	2.20 (d, 1.3)	14.4
21	1.72 (br s)	16.1	1.78 (br s)	16.5
22a	4.83 (br s)	108.8	1.16 (br s)	24.2
22b	4.65 (br s)			
23a	3.62 (d, 7.0)	84.6	3.64 (d, 7.0)	85.0
23b	3.44 (d, 7.0)		3.47 (d, 7.0)	
24	1.11 (s)	19.0	1.10 (s)	18.8
25	0.92 (s)	16.0	0.92 (s)	16.1

[a] *J* values are in parentheses and reported in Hz; chemical shifts are given in ppm; assignments were confirmed by COSY, 1D TOCSY, HSQC, and HMBC experiments. [b] These are overlapped signals.

at δ 3.80 with C-4, C-8, C-10, and C-23, and HMBC correlations of H_2-23 (δ 3.62 and 3.44) with C-3, C-24, C-5, and C-6 established the presence of a 6α,23-epoxide. The elucidation of the whole skeleton from the above subunits was achieved on the basis of HSQC and HMBC correlations, which also allowed the assignment of all the resonance in the ^{13}C NMR spectrum of the pertinent carbons (Table 1). The relative stereochemistry at C-4, C-5, C-6, C-9, and C-10 was established taking into account the *J* value for H-6, H-5, and H-9 (Table 2), and their axial orientation was indicated by a 2D-ROESY experiment showing ROE cross peaks among proton spatially related, particularly H-9 with H-5 and Me-24 and Me-25. This was confirmed by chemical shifts of the carbon atoms of rings A and B, which matched well with those of related di- and sesterterpenes.[19] The E configuration of Δ^{13} double bond was inferred from the upfield ^{13}C resonance at 16.3 ppm assigned to C-21.[20,21] To determine the C-16 absolute configuration, a modified Mosher's method was applied to a C-16 hydroxyl derivative of compound **1**.[22,23] Compound **1** was first treated with methyl lithium to give the butenolide-opened derivative, having a free C-16 hydroxyl residue (see Supporting Information).[24] Butenolide-opened derivative was then converted to (+)-*R*- and (−)-*S*-α-methoxy-α-(trifluoromethyl)phenylacetates (MTPA esters), which were subject to ^1H NMR analysis (see Supporting Information). On the basis of ^1HNMR data, the C-16 absolute configuration of compound **1** has been clarified to be R, being the same as salvialeucolide methyl ester, the configuration of which was established by X-ray diffraction analysis.[21]

Therefore, the structure of compound **1** was determined as 23,6α-epoxy-labd-8,13(14),17-trien-16(*R*),19-olide.

The molecular formula of compound **2**, $C_{25}H_{38}O_5$, was established by ^{13}C NMR and HRMS (obsd *m*/*z* 441.264 for $[M + Na]^+$ calcd *m*/*z* 441.262), indicating seven degrees of unsaturation.

The ^{13}C NMR of **2** contained resonances for all 25 carbons, while a DEPT experiment revealed the presence of five methyls, seven methylenes, seven methines, and six quaternary carbons.

COSY and 1D-TOCSY measurements showing coupling between H-14, H-15, H-16, H-18, and Me-21 established the spin system C-13−C-18. The linkage between C-15 and butenolide group was deduced by HMBC correlations; the signal at 4.75 (H-15) correlated to δ 170.7 (C-17) and δ 117.6 (C-18), and δ 4.99 (H-16) to 118.6 (C-18), δ 174.0 (C-19), 123.2 (C-14), and 143.9 (C-13). 1D-TOCSY and COSY experiments provided evidence for the presence in the molecule of segments H-9−H-11−H-12−H-14, H-1−H-3, and H-5−H-7. The elucidation of the whole skeleton from the above subunits was achieved on the basis of HSQC and HMBC correlations (Table 1).

The relative stereochemistry at C-4, C-5, C-6, C-8, C-9, and C-10 was established by taking into account the *J* value for H-6, H-5, and H-9, and their axial orientation was indicated by a 2D-ROESY experiment showing ROE cross between H-9 with H-5, and Me-22 with Me-24 and Me-25. The E configuration of Δ^{13} double bond was inferred from the upfield ^{13}C resonance 16.5 ppm assigned to C-21 and confirmed by ROE enhancement of H-15 proton on irradiation of Me-21.[20] The remaining feature needed to be fully established was stereochemistry at C-15 and C-16. The absolute configuration at C-15 of compound **2** was determined as in **1** using a modified Mosher's method.[22,23] In practice, there was a problem encountered with this approach: the C-15 OH group proved more reactive toward the elimination than the MTPA-esterification under a wide variety of conditions. During MTPA esterification, a dehydration took place with the formation of a conjugated double bond at the 15(16) position. Therefore, it was first necessary to reduce double bonds of the side chain to avoid the C-15 OH elimination. Compound **2** was converted by catalytic hydrogenation into the saturated derivatives, purified by TLC. The most abundant derivative of reduction was subject to NMR analysis. ^1H NMR and 1D-TOCSY experiments allowed complete assignments for all proton resonances of the side chain starting from the H-15 (δ 3.91) and H-16 (δ 4.36) signals. The (*S*)-configuration at C-15 was then derived by ^1H NMR analysis of the (*R*)-(+)- and (*S*)-(−)-MTPA esters (see Supporting Information).

To determine the C-16 absolute configuration, the lactone ring of **2** derivative was opened by alkaline hydrolysis, and the resulting hydroxyl acid was immediately methylated to give the butenolide-opened derivative, having a free C-16 hydroxyl residue (see Supporting Information).[24] The relative configuration of the 1,2-diol C-15/C-16 was determined with the following procedures. First of all, to obtain the relative configuration of C-15 and C-16, the acetonide derivative was prepared and the ^1H NMR chemical shifts of the acetonyl methyl groups were observed. The ^1H NMR signals of the acetonyl methyl groups appeared as six-proton singlet at ∼1.32 ppm, showing their equivalence and demonstrating that the vicinal diol at C-15/C-16 was *threo*.[25,26] Taking in account the established C-15 *S* absolute configuration and the C-15/C-16 *threo* relative configuration, it was possible to assess the *S*/*S*-configuration for C-15/C-16 diol. Consequently, C-16 absolute configuration of compound **2** has been clarified to be *S*.

Table 2. NMR Data of Compounds **3**−**6** (CD_3OD, 600 MHz)[a]

	3		**4**		**5**	**6**
pos	δ_H	δ_C	δ_H	δ_C	δ_C	δ_C
1a	1.73[b]	41.6	1.73[b]	41.9	41.8	41.6
1b	1.11 (ddd, 13.0, 12.5, 4.0)		1.06 (ddd, 13.0, 12.5, 4.0)			
2a	1.62[b]	18.0	1.76[b]	19.6	17.5	17.8
2b	1.48[b]		1.63[b]			
3a	1.80 (m)	33.3	1.62 [b]	32.3	32.0	32.1
3b	1.41[b]		1.46[b]			
4		42.5		44.8	44.6	44.8
5	1.58 (d,10.5)	61.0	1.54 (d,10.5)	57.8	57.6	57.7
6	4.43 (ddd, 11.0, 10.0, 4.8)	75.5	3.86 (ddd, 11.0, 10.0, 4.8)	74.5	74.3	74.5
7a	2.39 (dd, 12.0, 5.0)	48.6	2.30 (dd, 12.0, 4.8)	51.8	51.5	51.5
7b	1.63 (dd, 13.0, 12.0)		1.54 (dd, 13.0, 12.0)			
8		75.0		76.6	76.4	76.5
9	1.35 (dd, 6.0, 5.0)	60.9	1.20 (dd, 6.0, 5.0)	61.8	61.2	61.2
10		38.0		37.6	37.6	37.7
11a	1.70[b]	25.0	1.69[b]	24.3	23.8	23.5
11b	1.45[b]		1.47[b]			
12a	2.32 (ddd, 13.5,11.0, 3.5)	42.5	2.34 (ddd, 13.5,11.0, 3.5)	42.8	42.6	44.0
12b	2.10 (ddd, 13.5, 6.0, 3.5)		2.12 (ddd, 13.5, 6.0, 3.5)			
13		143.8		143.8	143.9	140.9
14	5.31 (d, 9.0)	123.5	5.27 (d, 8.7)	123.4	121.4	116.8
15a	4.77 (dd, 9.0, 2.5)	67.5	4.74 (dd, 8.7, 3.0)	67.7	67.0	31.0
15b						
16	4.95 (d, 2.5)	88.7	4.97 (d, 3.0)	88.9	88.8	86.0
17		170.5		170.6	170.7	170.5
18	5.92 (d, 1.0)	118.2	5.93 (d, 1.3)	118.7	116.6	117.4
19		174.0		176.0	174.0	174.0
20	2.20 (d, 1.0)	14.2	2.20 (d, 1.3)	14.4	14.3	13.6
21	1.78 (br s)	16.5	1.77 (br s)	16.7	16.5	16.3
22	1.23 (s)	23.9	1.14 (s)	24.4	24.0	24.6
23a		179.4	4.44 (s)	114.0	112.7	112.4
23b						
24	1.24 (s)	15.7	1.04 (s)	18.5	18.0	18.1
25	0.99 (s)	15.9	0.89 (s)	15.7	15.4	15.4
OEt					64.3	64.0
OEt					15.1	15.3

[a] *J* values are in parentheses and reported in Hz; chemical shifts are given in ppm; assignments were confirmed by COSY, TOCSY, HSQC, and HMBC experiments. [b] These are overlapped signals.

Thus, the structure of **2** was identified as 8α,15(*S*)-dihydroxy-23,6α-epoxy-labd-13(14),17-dien-16(*S*),19-olide.

The molecular formula of compound **3** $C_{25}H_{36}O_6$ was established by ^{13}C NMR and HRMS (obsd *m*/*z* 455.249 for $[M + Na]^+$ calcd *m*/*z* 455.251). Its NMR spectral data (Table 2) suggested that the structure of **3** resembled that of **2** but differed in the ring B. The ^1H and ^{13}C NMR spectra of compound **3** in respect of those of **2** showed the absence of the hydroxymethylene group (δ 3.64 and 3.47, δ 85.0). Comparison of chemical shifts with those of **2** suggested that the 6α,23-tetrahydrofuranic group was replaced by a 6α,23-lactone. In the ROESY spectrum of **3**, the correlation between Me-25, Me-24, and Me-22 confirmed that the stereochemistry of C-8 OH was α.

Thus, the structure of **3** was identified as 8α,15(*S*)-dihydroxy-labd-13(14),17-dien-23,6α-16(*S*),19-diolide.

The HRMS of **4** gave a quasimolecular ion at *m*/*z* 457.266 $[M + Na]^+$. The NMR data of **4** (Table 2) were similar to those of **2**, except that the hydroxyl-methylene group at C-23 (δ 3.64, and 3.47 in **2**) was replaced in **4** by a hemiacetal methine proton (δ 4.44 s), which was located at C-23 on the basis of the HMBC correlations of H-23 to C-6, C-5, C-24, and C-3, and H-6 to C-23, C-4, and C-5. The α-orientation of hydroxyl group at C-6 position was determined on the basis of chemical shift, the multiplicity and coupling costant values of the signal at δ 3.86 (ddd, 11.0, 10.0, 4.8, H-6), and from the resonaces of 24-Me and 25-Me, which were close to the resonances of 24- and 25-Me in related compounds.[19,21] The hemiacetal proton H-23 were assigned β-oriented on the basis of ROE interaction between H-23 and H-6. The decalin ring junction and side chain stereochemistry of **4** was identical to those of **2**.

On the above evidence, **4** was assigned as 8α,15(*S*),23α-trihydroxy-23,6α-epoxy-labd-13(14),17-dien-16(*S*),19-olide.

The ^1H and ^{13}C NMR spectra (Table 2) of compound **5** ($C_{27}H_{42}O_6$, HRMS obsd *m*/*z* 485.293 for $[M + Na]^+$ calcd *m*/*z* 485.288) were very similar to those of **4** except for the presence of an additional ethyl group (δ_c 15.1, δ_H 1.20, and δ_c 64.3, δ_H 3.77, and 3.44). Because the proton and carbon signals of the −CHOH at C-23 group was typically shifted (δ_H 4.58, δ_C 112.7 in **5** versus, δ_H 4.44, δ_C 114.0 in **4**), the C-23 position must be etherified by the ethyl group.

Thus the structure 8α,15(*S*)-dihydroxy,23α-*O*-ethyl-23,6α-epoxy-labd-13(14),17-dien-16(*S*),19-olide was assigned to compound **5**.

The HRMS of **6** gave a quasimolecular ion at *m*/*z* 469.318 $[M + Na]^+$. An examination of NMR spectra of **6** revealed side chain NMR signals similar to those of compound **1**. Data for the A- and B-rings strongly suggested that the identity of the bicyclic moiety of compound **6** is the same as that described for compound **5** (Table 2 and Experimental Section).

Therefore the structure 8α-hydroxy,23α-*O*-ethyl-23,6α-epoxy-labd-13(14),17-dien-16(*R*),19-olide was assigned to compound **6**.

The molecular formula of compound **7** $C_{25}H_{40}O_6$ was established by ^{13}C NMR and HRMS (obsd *m*/*z* 459.286 for $[M + Na]^+$ calcd *m*/*z* 459.272) indicating six degrees of unsaturation. Results obtained from 1D-TOCSY and COSY experiments established the connectivity of protons H-1−H-3, H-5−H-7,

Table 3. NMR Data of Compounds **7**−**12** (CD_3OD, 600 MHz)[a]

	7		**8**		**9**	**10**	**11**	**12**
pos	δ_H	δ_C	δ_H	δ_C	δ_C	δ_C	δ_C	δ_C
1a	1.76[b]	41.3	1.68[b]	40.6	41.5	42.0	41.8	40.2
1b	1.09 (ddd, 13.0, 12.5, 4.0)		1.02 (ddd, 13.0, 12.5, 4.0)					
2a	1.74[b]	18.5	1.75[b]	18.5	18.8	19.8	19.5	18.0
2b	1.52[b]		1.52[b]					
3a	1.36 [b]	38.6	1.36 [b]	38.7	42.1	36.5	36.6	39.0
3b	1.32[b]		1.32[b]					
4		40.3		38.1	34.6	45.0	44.6	45.9
5	1.25 (d,10.5)	58.4	1.22 (d, 10.5)	58.5	57.0	57.4	60.2	57.5
6	3.80 (ddd, 11.0, 10.0, 4.8)	67.8	3.78 (ddd, 11.0, 10.0, 4.8)	67.6	67.8	67.8	68.0	66.4
7a	2.14 (dd, 12.0, 4.8)	54.4	2.12 (dd, 12.0, 4.8)	54.7	54.5	54.1	54.3	54.1
7b	1.60 (dd, 13.0, 12.0)		1.58 (dd, 13.0, 12.0)					
8		74.5		74.0	77.0	75.1	75.6	74.6
9	1.24 (dd, 11.0, 3.5)	61.7	1.12 (dd, 11.0, 3.5)	61.5	62.0	61.7	61.3	61.6
10		37.9		38.0	38.0	37.8	37.8	38.8
11a	1.72[b]	25.4	1.57[b]	25.3	24.5	25.6	25.6	24.6
11b	1.34[b]		1.30[b]					
12a	2.23 (ddd, 13.5,11.0, 3.5)	43.5	2.16 (ddd, 13.5, 6.0, 3.5)	44.1	42.8	43.8	44.0	43.8
12b	2.09 (ddd, 13.5, 6.0, 3.5)		2.04 (ddd, 13.5,11.0, 3.5)					
13		143.4		140.9	143.6	143.4	141.2	143.5
14	5.29 (d, 8.8)	122.9	5.07 (dd, 8.0, 3.0)	116.7	123.4	123.0	117.1	123.0
15a	4.74 (dd, 8.8, 2.5)	67.6	2.70 (ddd, 14.0, 8.0, 6.0)	30.6	68.0	68.0	31.0	67.5
15b			2.44 (ddd, 14.0, 6.0, 2.0)					
16	4.96 (d 2.5)	88.6	5.05 m	86.0	89.0	88.9	85.8	88.9
17		170.5		171.0	170.6	170.8	171.6	170.4
18	5.92 (d 1.0)	118.5	5.87 (d, 1.3)	117.4	118.9	118.4	117.6	118.4
19		173.5		174.2	173.6	174.0	173.8	176.0
20	2.20 (d 1.0)	14.6	2.12 (d, 1.3)	13.6	14.6	14.0	13.8	14.0
21	1.79 (br s)	16.3	1.70 (br s)	16.3	16.8	16.7	16.1	16.7
22	1.18 (s)	25.1	1.18 (s)	24.5	24.5	25.0	24.3	24.6
23a	3.47 (d, 11.0)	75.3	3.46 (d, 11.0)	75.0	33.6	181.0	181.0	183.0
23b	3.24 (d, 11.0)		3.26 (d, 11.0)					
24	0.97 (s)	17.4	0.95 (s)	17.7	22.0	15.8	16.0	16.0
25	0.92 (s)	16.0	0.89 (s)	17.0	16.0	16.0	16.3	16.6
OMe								51.8

[a] *J* values are in parentheses and reported in Hz; chemical shifts are given in ppm; assignments were confirmed by COSY, TOCSY, HSQC, and HMBC experiments. [b] These are overlapped signals.

H-9−H-12, and H-12−H-16. The elucidation of the whole skeleton from the above subunits was achieved on the basis of HSQC and HMBC correlations, which also allowed the assignment of all the resonance in the ^{13}C NMR spectrum of the pertinent carbons (Table 3). The relative stereochemistry of **7** was identical to that of **2**.

On the above evidence, **7** was assigned as 6α,8α,15(*S*),23-tetrahydroxy-labd-13(14),17-dien-16(*S*),19-olide.

The HRMS of **8** gave a quasimolecular ion at *m*/*z* 443.291 $[M + Na]^+$. The ^1H NMR of **8** was very similar to those of **7**, suggesting the same skeleton. The main difference was the absence of signals at δ_H 4.74, δ_C 67.6 attributed in **7** to H-15, and the presence of signals at δ_H 2.73, δ_H 2.44, and δ_C 30.6. (Table 3). All data were indicative of the absence of C-15 OH group in compound **8**.

Thus, **8** was established as as 6α,8α,23-trihydroxy-labd-13(14),17-dien-16(*R*),19-olide.

The ^1H and ^{13}C NMR spectra (Table 3 and Experimental Section) of compound **9** ($C_{25}H_{40}O_5$) was very similar to those of **7**, except for the presence of an additional methyl group (δ_c 33.6, δ_H 1.18) instead of a hydroxymethylene function (δ_c 75.3, δ_H 3.47, and 3.24).

Therefore compound **9** was characterized as 6α,8α,15(*S*),trihydroxy-labd-13(14),17-dien-16(*S*),19-olide.

Compounds **10** and **7** exhibited closely comparable spectroscopic data, except for the presence of signal at 181.0 ppm in the ^{13}C NMR spectrum of compound **10**, corresponding to a carboxyl group and the lack of the signal at 75.3 ppm for a $-CH_2OH$-23 group observed in the ^{13}C NMR spectra of **7**. In addition the resonances of C-3, C-4, C-5, and C-24 confirmed the presence of a carboxyl group at C-4 (Table 3).[27]

On the basis of these data, compound **10** was 6α,8α,15(*S*)-trihydroxy-23-carbossi-labd-13(14),17-dien-16(*S*),19-olide.

Compound **11** gave the molecular formula, $C_{25}H_{36}O_6$, as deduced from the ESIMS and from NMR spectroscopic analysis. An examination of NMR spectra of this compound revealed NMR signals of side chain protons and carbons similar to those of compound **8**. Data for the A- and B-rings strongly suggested that the identity of the bicyclic moiety of compound **11** is the same as that described for compound **10** (Table 3).

On the basis of these data, compound **11** was 6α,8α-dihydroxy-23-carbossi-labd-13(14),17-dien-16,19-olide.

NMR data of **12** ($C_{26}H_{40}O_7$, HRMS obsd *m*/*z* 487.270 for $[M + Na]^+$ calcd *m*/*z* 487.267) compared with those of **10** showed that the only difference was the presence of a $-COOCH_3$ group in **12** instead of a −COOH group in **10** (Table 3).[28] Hence, **12** was established as 6α,8α,15(*S*)-trihydroxy-23-carbossimethyl-labd-13(14),17-dien-16(*S*),19-olide.

Compound **13** ($C_{25}H_{38}O_6$) showed an $[M + Na]^+$ ion at *m*/*z* 457.265. Comparison of the NMR spectral data of compound **13** with those of **9** showed these to be identical in the side chain part but different in the rings portion. In particular, hydrogen and carbon NMR signals due to the atoms of A- and B-rings were shifted somewhat. The NMR spectra of **13** contained one less methyl signal and one more aldehydic group signal than those of **9**, suggesting that one of Me groups was replaced by an aldehydic group in **13**. The most significant features of the ^{13}C NMR spectrum of

Table 4. NMR Data of Compounds **13**−**16** (CD_3OD, 600 MHz)[a]

	13		**14**	**15**		**16**
pos	δ_H	δ_C	δ_C	δ_H	δ_C	δ_C
1a	1.75[b]	40.0	40.0	1.70[b]	41.3	40.9
1b	1.12 (ddd, 13.0, 12.5, 4.0)			1.05 (ddd, 13.0, 12.5, 4.0)		
2a	1.74[b]	17.5	18.0	1.52[b]	18.5	18.0
2b	1.63[b]			1.36[b]		
3a	1.39[b]	32.9	32.6	1.26[b]	38.6	32.9
3b	1.10 (m)			1.36		
4		54.3	54.6		39.0	53.0
5	1.61 (d,10.5)	57.5	57.3	1.25 (d, 11.0)	58.4	57.0
6	3.64 (ddd, 11.0, 10.0, 4.8)	66.3	66.5	3.78 (ddd, 11.0, 10, 4.8)	67.8	66.3
7a	2.13 (dd, 13.5, 4.8)	54.0	53.8	2.53 (dd, 13.0, 4.8)	46.3	46.0
7b	1.60 (dd, 13.5, 12.0)			1.99 (dd, 13.0, 12.0)		
8		74.9	75.0		147.6	148.8
9	1.24 (dd, 11.0, 3.5)	61.7	61.8	1.87 (dd, 11.0, 3.5)	57.6	57.8
10		38.9	3806		38.8	37.8
11a	1.64[b]	24.3	24.3	1.66[b]	23.7	24.3
11b	1.40[b]			1.33[b]		
12a	2.30 (ddd, 13.5,11.0, 3.5)	43.8	44.1	2.20 (ddd, 13.5,11.0, 3.5)	43.0	42.8
12b	2.11 (ddd, 13.5, 6.0, 3.5)			2.02 (ddd, 13.5, 6.0, 3.5)		
13		143.3	140.6		143.9	143.8
14	5.32 (d, 8.7)	123.0	117.0	5.29 (d, 9.0)	122.6	123.4
15a	4.74 (dd, 8.7, 3.0)	67.5	31.0	4.79 (dd, 9.0, 2.0)	66.8	67.7
15b						
16	4.96 (d, 3.0)	88.7	85.9	4.96 (d, 2.0)	88.6	88.9
17		171.0	171.1		170.5	170.6
18	5.93 (d, 1.2)	118.3	117.4	5.96 (d, 1.3)	117.6	118.7
19		176.3	174.0		174.5	176.0
20	2.21 (d, 1.2)	14.2	13.6	2.20	14.6	14.4
21	1.79 (br s)	16.5	16.3	1.79 (s)	16.5	16.7
22a	1.19 (s)	24.7	24.6	4.88 (s)	109.0	108.6
22b				4.63 (s)		
23	9.52 (s)	209.0	209.2	3.49 (d, 12.0)	75.6	209.0
23				3.30 (d, 12.0)		
24	1.18 (s)	13.8	13.8	1.00 (s)	17.6	13.8
25	0.93 (s)	16.6	16.7	0.88 (s)	16.0	16.6

[a] *J* values are in parentheses and reported in Hz; chemical shifts are given in ppm; assignments were confirmed by COSY, TOCSY, HSQC, and HMBC experiments. [b] These are overlapped signals.

13, which suggested placement of the 23-Me, were downfield shifted as exhibited by C-4, and the upfield shift was exhibited by C-3, C-5 and C-24 in comparison with the same carbon resonances in sesterterpene skeleton bearing a 23-Me (Table 4).[29] 1D-ROESY experiments supported the α-orientation of 23-CHO group: irradiation of 24-Me at δ 1.18 (3H, s) affected the signals of 25- and 22-Me groups.

Thus **13** was determined to be 6α,8α,15(*S*)-trihydroxy-23-*oxo*-labd-13(14),17-dien-16(*S*),19-olide.

Compound **14** ($C_{25}H_{38}O_5$) showed an $[M + Na]^+$ ion at *m*/*z* 441.268. Its ^1H NMR spectrum, when compared to that of **13**, showed the absence of carbinol signal attributed in **13** to H-15 and the occurrence of two signals at δ 2.75 and 2.41 ascribable to a methylene group.

Therefore compound **14** was characterized as 6α,8α-dihydroxy-23-*oxo*-labd-13(14),17-dien-16(*R*),19-olide.

Compound **15** ($C_{25}H_{38}O_5$) showed an $[M + Na]^+$ ion at *m*/*z* 441.270. Comparison of the NMR spectral data of compound **15** with those of **7** showed these to be different in the B-ring portion. The most significant features of the NMR spectra of **15** were upfield shifted as exhibited by C-9 and C-7, and downfield shifted as exhibited by H-9 and H_2-7 (Table 4), which indicated the presence of $\Delta^{8,22}$ exocyclic methylene group in compound **15**.[30]

Therefore compound **15** was characterized as 6α,15(*S*),23-trihydroxy-labd-8(22),13(14),17-trien-16(*S*),19-olide.

Compound **16** had the molecular formula $C_{25}H_{36}O_5$, as deduced from HRMS (observed *m*/*z* 439.251 $[M + Na]^+$). The ^1H and ^{13}C NMR spectra (Table 4 and Experimental Section) of compound **16** were very similar to those of **15**, except for the hydroxymethylen group at C-4 in **15**, which was replaced by a aldehydic group in compound **16**. All ^1H and ^{13}C NMR assignments were confirmed by analysis of 2D NMR spectra.

Therefore compound **16** was characterized as 6α,15(*S*)-dihydroxy-23-*oxo*-labd-8(22),13(14),17-trien-16(*S*),19-olide.

The molecular formula of compound **17** was established as $C_{25}H_{38}O_5$ by HRMS ($[M + Na]^+$, 441.269), indicating seven unsaturations in the molecule. An NMR study of this compound revealed signals of A- and B-rings similar to those of **7**. The side chain NMR data (Table 5) indicated the presence of an α,β,γ-unsaturated five-membered lactone ring (δ_C 115.9, 151.2, 164.8, 172.0, and δ_H 6.0). Further resonances in the ^{13}C NMR spectrum at δ_C 147.9, 118.7, 109.3 ppm indicated the presence of two carbon−carbon double bonds, ^1H NMR spectrum and UV 350 nm suggested the presence of a trienone system.[31] A combination of 2D NMR experiments delineated, for the side chain, three main connectivities: the first one comprised C-11, C-12, and C-14, the second was C-14, C-15, and C-21, and the third was C-20 and C-18 (Table 5). Key correlation peaks were observed between Me-21 and C-12, C-13, C-14, and C-15; Me-20 and C-15, C-16, C-18, and C-17; H-14 and C-21, C-12, and C-16; H-15 and C-13, C-17, C-19, and H-18, and C-16, C-20. The coupling constant values $J_{14,15} = 11.6$ Hz suggested the *Z*-geometry.

On the basis of these data, compound **17** was 6α,8α,23-trihydroxy-labd-13(14),15,17-trien-16,19-olide.

Compound **18** ($C_{25}H_{36}O_6$) showed an $[M + Na]^+$ ion at *m*/*z* 455.249. Compounds **18** and **17** exibited comparable spectroscopic data, except for the presence of signal at 181.5 ppm corresponding to a carboxyl group and the lack of the signal at

Table 5. NMR Data of Compounds **17**−**21** (CD_3OD, 600 MHz)[a]

	17		**18**	**19**	**20**	**21**	
pos	δ_H	δ_C	δ_C	δ_C	δ_C	δ_H	δ_C
1a	1.76[b]	41.8	42.0	40.2	41.6	1.77[b]	42.0
1b	1.06 (ddd, 13.0, 12.5, 4)					1.04 (ddd, 13.0, 12.5, 4.0)	
2a	1.74[b]	19.8	19.5	17.7	18.6	1.75[b]	19.6
2b	1.52[b]					1.64[b]	
3a	1.36 (m)	38.2	36.3	33.0	33.6	1.63[b]	32.4
3b	1.24[b]					1.48 (m)	
4		40.3	45.0	53.0	42.5		44.3
5	1.28 (d,11.0)	58.4	59.2	57.7	61.0	1.54 (d,10.5)	57.8
6	3.82 (ddd, 11.0, 11.5, 3.5)	67.8	66.9	66.3	75.5	3.86 (ddd, 11.0, 11.5, 3.5)	74.8
7a	2.14 (dd, 13.0, 3.0)	54.4	54.1	54.1	48.6	2.31 (dd, 13.0, 3.0)	51.9
7b	1.60 (dd, 13.0, 11.5)					1.56 (dd, 13.0, 11.5)	
8		74.8	74.8	73.8	74.9		74.9
9	1.16 (dd, 11.0, 3.5)	62.2	61.7	61.7	60.9	1.20[b]	62.2
10		38.0	38.0	38.0	38.0		38.0
11a	1.72[b]	23.8	24.5	24.5	25.0	1.70[b]	24.1
11b	1.50[b]					1.53[b]	
12a	2.51 (ddd, 12.5, 11.5, 3.5)	42.9	43.8	43.6	43.5	2.51 (ddd, 12.5, 12.0, 3.5)	43.6
12b	2.32 (ddd, 12.5, 5.0, 3.5)					2.32 (ddd, 12.5, 5.0, 3.5)	
13		147.9	148.0	148.0	148.2		147.8
14	6.42 (dd, 11.8, 1.2)	118.7	118.6	118.8	118.2	6.40 (dd, 11.6, 1.2)	119.0
15	6.28 (d, 11.8)	109.3	109.0	109.5	108.4	6.29 (d, 11.6)	109.2
16		151.2	151.0	151.2	151.5		152.0
17		164.8	164.2	164.6	164.5		164.6
18	6.00 (br s)	115.9	115.6	115.6	115.2	5.98 (s)	115.9
19		172.0	171.8	171.6	171.8		171.8
20	2.26 (br s)	11.0	11.3	11.3	11.8	2.26 (s)	11.0
21	1.98 (d, 1.2)	17.0	17.3	17.5	17.4	1.98 (d, 1.2)	17.0
22	1.24 (s)	24.4	24.7	24.7	23.9	1.14 (s)	24.4
23a	3.47 (d, 11.5)	75.3	181.5	209.0	176.0	4.47 (s)	114.2
23b	3.25 (d, 11.5)						
24	0.99 (s)	17.4	15.6	13.8	15.6	1.06 (s)	18.4
25	0.94 (s)	16.9	16.3	16.7	15.5	0.94 (s)	15.9

[a] *J* values are in parentheses and reported in Hz; chemical shifts are given in ppm; assignments were confirmed by COSY, TOCSY, HSQC, and HMBC experiments. [b] These are overlapped signals.

75.3 ppm for a $-CH_2OH$-23 group observed in the ^{13}C NMR spectrum of **18**. The resonances of C-3, C-4, C-5, and C-24 confirmed the presence of a carboxyl group at C-4 (Table 5 and Experimental Section).

On the basis of these data, compound **18** was 6α,8α-dihydroxy-23-carbossi-labd-13(14),15,17-trien-16,19-olide.

Compound **19** ($C_{25}H_{36}O_5$) showed an $[M + Na]^+$ ion at *m*/*z* 439.253. Comparison of the NMR spectral data of compound **19** with those of **17** showed these to be identical in the side chain portion but different in the rings portion. Data for the A- and B-rings strongly suggested that the identity of the bicyclic moiety of compound **19** is the same as that described for compound **13** (Table 5 and Experimental Section).[29]

Therefore compound **19** was characterized as 6α,8α-dihydroxy-23-*oxo*-13(14),15,17-trien-16,19-olide.

Compound **20** gave the molecular formula $C_{25}H_{34}O_5$, as deduced from the ESIMS and from NMR spectroscopic analysis. An examination of NMR spectra of this compound revealed signals of side chain protons and carbons similar to those of compound **17**. Data for the A- and B-rings strongly suggested that the identity of the bicyclic moiety of compound **20** is the same as that described for compound **3** (Table 5 and Experimental Section).

Therefore, compound **20** was determined to be 8α-hydroxy-labd-13(14),15,17-trien-6α,23-16,19-diolide.

Compound **21** gave the molecular formula $C_{25}H_{36}O_5$, as deduced from the ESIMS and from NMR spectroscopic analysis. An examination of NMR spectra of this compound revealed signals of protons and carbons attributed to the side chain of compound **17**. Data for the A- and B-rings strongly suggested that the identity of the bicyclic system of compound **21** was the same as that described for compound **4** (Table 5 and Experimental Section).

Therefore, compound **21** was determined to 8α-23-dihydroxy-23,6α-epoxy-labd-13(14),15,17-trien-16,19-olide.

Compounds **22** and **23** yielded a pseudomolecular ion peak in the positive HRMS spectrum at *m*/*z* 475.271 $[M + Na]^+$, consistent with a molecular formula of $C_{25}H_{40}O_7$.

NMR spectral data of compound **22** suggested that the structure of **22** resembled that of compound **7** but differed in side chain. The carbonyl resonance at C-19 (172.0 ppm) was assigned based on HMBC correlations between H-18 and C-20 and C-19, and between Me-20 and C-19. A signal at δ 2.14 was consistent with the presence of a methyl group at C-17, and this was supported by HMBC correlations between Me-20 and C-17; Me-20 also showed long-range COSY correlations to H-18 (δ 5.92), supporting the presence of an α,β-unsaturated butenolide moiety. Results obtained from 1D TOCSY and COSY experiments established the correlations of protons H-9−H-11−H-12 and H-14−H-16, confirmed by HMBC cross peaks between H-12 (δ 2.30) and C-9 (δ 61.7), and C-14 (δ 76.6) and C-21 (δ 113.2). The A- and B-rings stereochemistry of **22** was identical to those of compound **7**.[32]

The NMR data of compound **23** was quite similar to that of **22** (Table 6), the main differences being in the resonances of H_2-12, H-14, H-15, H-16, Me-21, and C-13, C-14, and C-15. This evidence suggested the presence of a C-14/C-15 epimer. To obtain the relative configuration of 1,2-diol C-14/C-15 in **22** and **23**, the acetonide derivative was prepared and the ^1H NMR chemical shift of the acetonyl methyl groups was observed. The ^1H NMR signals of the acetonyl methyl groups in **22** appeared as six-proton singlet at ∼1.31 ppm, showing

Table 6. NMR Data of Compounds **22**−**24** (CD_3OD, 600 MHz)[a]

	22		**23**		**24**
pos	δ_H	δ_C	δ_H	δ_C	δ_C
1a	1.76[b]	40.6	1.72[b]	41.0	40.2
1b	1.09 (ddd, 13.0, 12.5, 4.0)		1.05 (ddd, 13.0, 12.5, 4.0)		
2a	1.74[b]	18.5	1.68[b]	18.5	18.2
2b	1.52[b]		1.52 (m)		
3a	1.36 [b]	38.8	1.37 (m)	39.1	33.0
3b	1.24[b]		1.27[b]		
4		39.7		39.8	52.0
5	1.28 (d,11.0)	58.5	1.25 (d, 11.0)	58.5	57.9
6	3.82 (ddd, 11.0, 11.5, 3.5)	67.7	3.80 (ddd, 11.0, 11.5, 3.5)	67.9	66.5
7a	2.16 (dd, 13.0, 3.0)	54.6	2.15 (dd, 13.0, 3.0)	54.8	54.1
7b	1.60 (dd, 13.0, 11.5)		1.59 (dd, 13.0, 11.5)		
8		74.4		74.6	73.9
9	1.24[b]	61.7	1.22[b]	61.9	61.5
10		37.8		38.2	38.0
11a	1.70[b]	25.0	1.72[b]	25.0	25.4
11b	1.50[b]		1.48[b]		
12a	2.30 (ddd, 12.5, 11.5, 3.5)	34.5	2.36 (ddd, 12.5, 11.5, 4.5)	35.5	35.2
12b	2.23 (ddd, 12.5, 5.0, 3.5)		2.17 ddd 12.5, 5.0, 4.5)		
13		151.1		152.0	151.3
14	4.19 (d, 9.0)	76.6	4.21 (d, 8.8)	77.3	76.4
15	3.82 (br d, 9.0)	70.4	3.88 (dd, 8.8, 1.2)	72.5	72.3
16	5.40 (br s)	85.7	4.94 (d, 1.2)	86.9	86.8
17		171.5		171.8	171.3
18	5.92 (d, 1.3)	117.5	5.89 (d, 1.2)	117.6	117.6
19		172.0		172.0	172.0
20	2.14 (d, 1.3)	13.5	2.14 (d, 1.2)	13.7	13.5
21a	5.14 (s)	113.2	5.12 (s)	114.2	112.9
21b	5.05 (s)		5.22 (s)		
22	1.24 (s)	24.8	1.21 (s)	24.8	24.7
23a	3.47 (d, 11.5)	75.2	3.46 (d, 11.5)	75.6	209.0
23b	3.25 (d, 11.5)		3.23 (d, 11.5)		
24	0.99 (s)	17.7	0.96 (s)	17.9	13.3
25	0.94 (s)	16.8	0.92 (s)	17.3	17.0

[a] *J* values are in parentheses and reported in Hz; chemical shifts are given in ppm; assignments were confirmed by COSY, TOCSY, HSQC, and HMBC experiments. [b] These represent overlapped signals.

their equivalence and demonstrating that the diol at C-14/C-15 was *threo*, while the acetonyl methyl signals in **23** appeared as two separated three-proton singlets at δ 1.30 and 1.56, demonstrating that the configuration of the 1,2 diol in **23** was *erythro*.[33]

Therefore, the structure of compounds **22** and **23** were determined as 6a,8a,23,14,15-*threo*-pentahydroxy-labd-13(21),17-dien-16,19-olide and as 6a,8a,23,14,15-*erythro*-pentahydroxy-labd-13(21),17-dien-16,19-olide, respectively.

Positive HRMS spectrum of **24** showed a single ion peak at 473.260 $[M + Na]^+$, indicative of the molecular formula $C_{25}H_{38}O_7$. Analysis of the COSY and HSQC experiments of **24** indicated the presence of the same partial structure in the side chain as that of **22** but showed that rings A and B were different. The NMR spectra of **24** contained one less hydroxymethylene group and one more aldehydic group (δ_H 9.5, δ_C 209.0) than those of **22**, suggesting that in **24** the hydroxymethylen group was replaced by an aldehydic group.[29] The stereochemistry of C-14/C-15 diol was determined as compounds **22** and **23.** Therefore, compound **24** was determined as 6a,8a,14,15-*threo*-tetrahydroxy-23-*oxo*-labd-13(21),17-dien-16,19-olide.

The copresence of compounds **4** and **13** and **19** and **20** in *S. dominica* extracts was assessed by the use of LC/MS^n analysis performed on crude acetone extract. Indeed, MS and MS/MS data allowed identification of compounds carrying an aldehyde, an acetal, or an emiacetal group (see Supporting Information).

Cytoxicity. All the isolated compounds were tested on their cytotoxic activity on three cell lines (MCF-7 human breast adenocarcinoma, J774.A1 murine monocyte/macrophagy, HEK293 human epithelial kidney) but showed nonsignificant activity at the doses evaluated (>100 μM).

Chemical Proteomics. One of the most versatile methods to profile cellular targets of selected drug candidates is compound-immobilized affinity chromatography. The procedure involves the compound immobilization on a solid support through a spacer arm and the use of this matrix as a bait to fish for interacting proteins in a cellular lysate or tissue extract.[34,35] The power of affinity chromatography combined with advances in protein identification by sensitive and high-throughput mass spectrometric analysis offers huge potential to find out previously unrecognized activities and potential therapeutic applications.

To investigate the biological activities of sestertepenes from *S. dominica*, an affinity column with covalently bound compound **13** was prepared in order to identify its potentially binding proteins. Literature data suggested that pharmacological activity of **1**−**24** could depend on the presence of α,β-unsaturated lactone moiety; therefore, compound **13** was covalently coupled to the controlled pore glass (CPG) beads exploiting its aldehyde function at C-23.

In characterizing binding partners for a small molecule by MS, the major challenge is to identify bona fide interacting partners because very high sensitivity of MS analysis can permit identification of almost all proteins, even contaminants present at very low levels in the sample, thus the use of a negative control is crucial. Total protein extracts were derived from MCF-7, as this breast cancer cell line was already used to test biological activities of sesterterpenes.[20] An equal amount of cell lysate was loaded on the covalently coupled beads and on unmodified beads in parallel to discriminate between proteins specific interacting with compound **13** and aspecific background.[36] Both samples underwent several washing steps, and proteins retained by loaded and unloaded beads were eluted by

Table 7. Mass Spectrometry Analysis of Tryptic Digest of Gel band at 45 kDa

experimental MW (Da)	identification	theoretical MW (Da)	error (ppm)	MS/MS fragments (Da)
728.36				
982.50	TTL1(457−464)	982.491	10	
1044.53	TTL1 (104−113)	1044.524	6	884.4; 728.4; 657.4; 528.3; 457.3; 102.1
1066.51	TTL1 (275−283)	1066.494	15	821.4; 764.3; 633.3; 532.3; 120.1; 102.1
1202.53	TTL1 (133−144)	1202.524	5	1045.4; 930.4; 802.3; 660.3; 603.2; 474.2; 248.1
1235.58				
1348.71				
1495.68	TTL1 (412−423)	1495.665	10	
1516.82				
1573.76	TTL1 (118−132)	1573.758	1	1501.7; 1400.7; 1372.7; 1301.6; 1173.5; 1172.6; 1101.6; 929.5; 699.4
1947.91	TTL1 (293−307)	1947.882	14	1847.1; 1776.0; 1714.8; 1586.7; 1514.7; 1472.7; 1359.6; 1212.5; 986.4; 857.4
2071.96	TTL1 (205−225)	2071.952	4	

complete denaturation, using Laemmli buffer. The proteins collected from each column were then analyzed by SDS-PAGE. Two protein bands showing an apparent molecular weight of 32 and 45 kDa, respectively, were detected only in the lane with proteins coming from **13**-loaded column. These bands were excised from the gel, digested with trypsin, and the resulting peptide mixtures were analyzed by nano-LC/MS/MS. Two gel pieces excised from the corresponding portions of the control lane were subjected to an analogous treatment, and the MS signals present in the negative control were subtracted from those obtained for the **13**-loaded elution.

Specific *m*/*z* values obtained for each protein band and, if available, the corresponding MS/MS data, were used to identify the proteins. Both Mascot and Protein prospector were used as search engines. The gel band at 45 kDa was successfully attributed to the human tubuline−tyrosine ligase (TTL) (SwissProt code: TTL_HUMAN). Eight out of the 12 specific *m*/*z* values used in protein search were compatible with tryptic peptides from this protein (mass accuracy between 1 and 15 ppm), and for five of these peptides, it was possible to obtain MS/MS spectra confirming their sequences (Table 7). These data permitted an unambiguous identification of TTL.

Unfortunately, the second band was not identified, possibly because of the low resolution power of the electrophoresis method and for the presence of unspecific contaminant proteins.

Surface Plasmon Resonances (SPR) Studies. Surface plasmon resonance allows measurement of kinetic and thermodynamic parameters of ligand−protein complex formation.[37] An SPR based binding assay as implemented with Biacore technology was, therefore, used to investigate the interactions between TTL and compounds **1**−**24**. This assay allowed us to verify the affinity of compounds **1**−**24** toward the investigated protein and to assess how these compounds associate and dissociate from the protein in real time, giving a more detailed view about their interaction with TTL. Moreover, on the basis of the SPR data, some structure−activity relationships evaluation was performed. An example of results obtained in these experiments is shown in Figure 2. Eighteen out of the 24 tested compounds efficiently interacted with the immobilized protein, as demonstrated by the concentration dependent responses and by the clearly discernible exponential curves during both the association and dissociation phases. Compounds **1**−**24** were also injected on immobilized bovine serum albumin (BSA) to evaluate possible unspecific bindings, and none of them interacted with this protein (data not shown).

The good quality of the acquired sensorgrams allowed fitting the curves to a single-site bimolecular interaction model (A + B = AB): using this approach, kinetic and thermodynamic parameters for each complex formation were achieved. Each constant was calculated fitting at least 10 curves, obtained injecting twice the investigated sesterterpenes at five different concentrations ranging from 0.05 to 10 μM. The constant values calculated for each compound are listed in Table 8. On the basis of these data, some evaluation concerning the effect of structural features of *S. dominica* sesterterpenes on their affinity for TTL protein was achieved. Comparison of the obtained pseudothermodynamic dissociation constants for compounds **1**−**24** (Table 8) clearly showed that a side chain is crucial for the TTL/

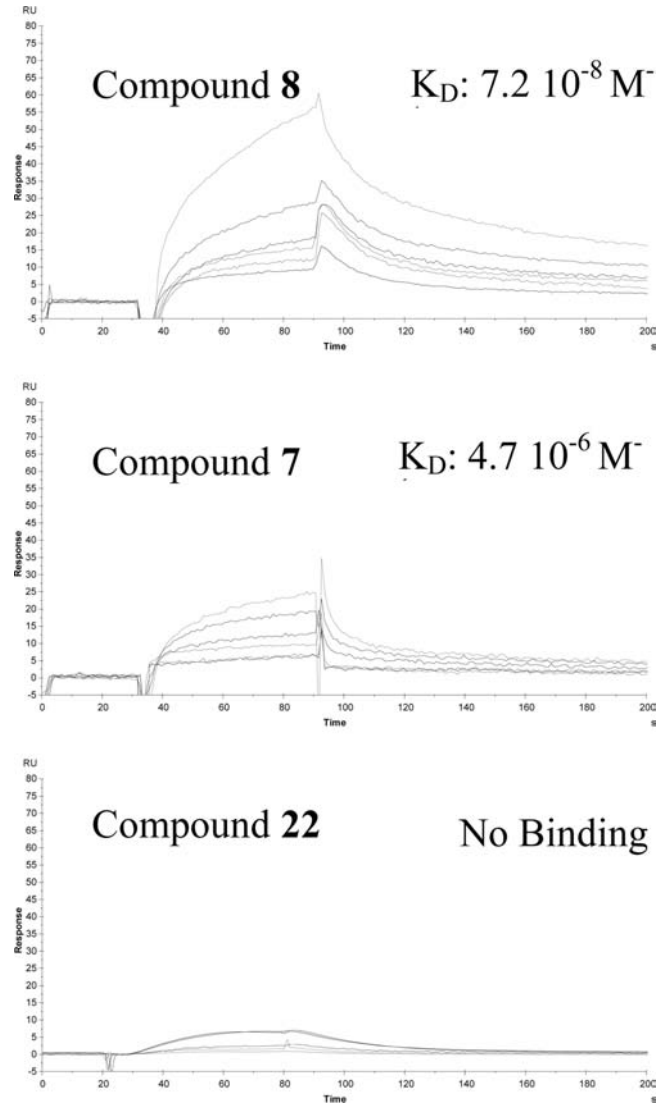

Figure 2. Sensorgrams obtained by injecting different concentrations (from 0.05 to 10 μM) of compound **7**, **8**, or **22** on TTL.

Table 8. Pseudothermodynamic Dissociation Constants Measured by SPR Studies for the Interaction between Compounds **1**−**24** and TTL

compd	K_D (M)
1	8.7×10^{-6}
2	no binding
3	no binding
4	2.1×10^{-4}
5	9.6×10^{-7}
6	7.3×10^{-8}
7	4.7×10^{-6}
8	7.2×10^{-8}
9	no binding
10	3.0×10^{-6}
11	0.7×10^{-8}
12	6.2×10^{-6}
13	3.0×10^{-6}
14	8.1×10^{-7}
15	2.0×10^{-6}
16	3.3×10^{-6}
17	1.1×10^{-7}
18	9.3×10^{-8}
19	2.0×10^{-7}
20	1.5×10^{-7}
21	4.8×10^{-7}
22	no binding
23	no binding
24	no binding

sesterterpenes interaction. Of 24 sesterterpenes tested compounds **6**, **8**, **11**, and **18** showed the best K_D, contrasted with the inactivity of compounds **9**, and **22**−**24**, which differed in the presence of one or two free −OH group at C-14 and C-15 of side chain. The presence of a $\Delta^{15,16}$ slightly reduces affinity for the enzyme, as can be deduced comparing the K_D values measured for **8** and **17** or those measured for **14** and **19**. All these data indicated that a side chain carring a $\Delta^{13,14}$ double bond and C-15 methylene group are required for activity.

On the other hand, different substituents at A- and B- rings have a negligible effect on the affinity of sesterterpenes for TTL, thus suggesting a secondary role for the bicyclic portion in the interaction. However, the occurrence of 23,6α-epoxy ring (compounds **1**, **2**, **4**, and **22**) or of 23,6α-γ-lactone ring (compounds **3** and **20**) clearly reduces the efficiency of the interaction, possibly because of the lower solubility. This hypothesis was partially confirmed by SPR data of **9**: this compound, having two methyl groups at C-4, completely failed to bind to the immobilized protein.

Inhibition of TTL Activity. Structural and functional features of microtubles are associated to different post-translational modifications on the α- and β-tubulin protein subunits.[38] Among the other modifications, α-tubulin undergoes to cyclic removal and readdition of the C-terminal tyrosine residue via a tubulin-specific carboxypeptidase (TCP) activity and a tubulin−tyrosine ligase (TTL). The detyrosinated α-tubulin (glu-tubulin) is also subject to further proteolytic cleavage of the penultimate glutamate residue to give a "non-tyrosinatable" form of α-tubulin, indicated as Δ2-tubulin, that accumulates when TTL activity is compromised.[39] To evaluate the in cell effects of sesterterpenes on TTL activity, we performed experiments incubating MCF-7 cells with 100 μM compound **11** (the most active compound from SPR studies, $K_D = 4.7 \times 10^{-8}$ M) for 24 and 48 h and then analyzing by western blot Δ2-tubulin levels in these conditions. Cell viability at these times and concentrations of incubations was assessed by MTT assay (see Supporting Information). Our data (Figure 3) showed a sensible increase of the characteristic multiband signal given by Δ2-tubulin

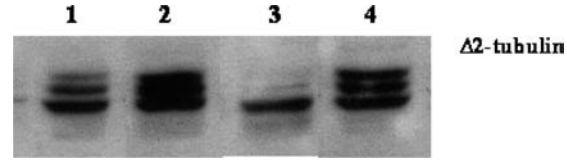

Figure 3. Western blot analysis of Δ2-tubulin in MCF-7 cell extract incubated (lanes 2 and 4) or not (lanes 1 and 3) with 100 μM compound **11**, after 24 h (lanes 1and 2) or 48 h (lanes 3 and 4).

antibody, indicating that compound **11** can penetrate the membrane and act as an inhibitor of TTL inside the cancer cell.

Conclusions

In summary, we have fully characterized 24 new sesterterpenes derivatives form the aerial parts of *Salvia dominica*. Sesterterpenes show different interesting biological activities, including cytotoxicity against cancer cells;[20,40,41] therefore, a multiple-approach-based study was performed to identify possible molecular target(s) of compounds **1**−**24** among breast cancer cell proteins, leading to the identification of TTL. This is an enzyme involved in a peculiar post-translational modification of α-tubulin, one of the microtubule building blocks: α-tubulin undergoes a process by which the C-terminal tyrosine is removed and readded.[42] This cycle of detyrosination and tyrosination is evolutionarily conserved[43] and is catalyzed by the activity of TTL[44] and TCP.[45]

While the detyrosination/tyrosination cycle of α-tubulin has been studied extensively,[38] the precise biological function of this highly specific protein modification has remained elusive. However, evidence suggest that the detyrosination/tyrosination cycle of α-tubulin may be linked, in some cell types, to cell division and proliferation.[46] There are suggestions that the carboxyl-terminus of α-tubulin may be involved in the control of cell cycle progression[47] and in the association/disassociation of motor proteins during cell division.[48] TTL is frequently suppressed during tumor progression, with resulting accumulation of Glu-tubulin in tumor cells.[16] Moreover, a vital role for TTL was demonstrated in the control of neuronal organization.[14]

Our chemical proteomics and SPR data demonstrated a selective affinity of sesterterpenes **1**−**24** for TTL and in cell biochemical analysis indicated an inhibition activity toward the enzyme. This class of compounds can constitute useful tools to investigate the detyrosination/tyrosination cycle of α-tubulin in order to deeply understand its role in the regulation of duplication and proliferation of different cell types. Thus, the present series of sesterterpenes has allowed us to determinate the critical role of side chain, the negative effect of any hydroxylation at side chain, and the differential effect of substituent at C-23 and C-6 positions. These findings on the structure−activity relationship should provide information for the future design of TTL inhibitors.

3. Experimental Section

3.1. General Experimental Procedures. Optical rotations were measured on a Perkin-Elmer 241 polarimeter equipped with a sodium lamp (589 nm) and a 1 dm microcell. IR measurements were obtained on a Bruker IFS-48 spectrometer. UV measurements were obtained on Beckman DU530 UV−vis Life Science spectrophotometer. NMR experiments were performed on a Bruker DRX-600 spectrometer equipped with a Bruker 5 mm TCI CryoProbe at 300 K. All NMR spectra were acquired in CD_3OD (99.95%, Sigma-Aldrich), and standard pulse sequences and phase cycling were used for DQF-COSY, HSQC, HMBC, and ROESY spectra. The ROESY spectra were acquired with $t_{mix} = 400$ ms. The NMR data were

processed on a Silicon Graphic Indigo2 workstation using UXNMR software. High resolution mass spectra were acquired on a Q-Tof Premier instrument (Waters, Milford, MA) equipped with a nanospray ion source; to achieve high accuracy mass measurements, both external and internal calibrations of the spectrometer were performed using quercetin (molecular mass 302.0427) or amentoflavone (molecular mass 538.0900) as standards. ESIMS and LC/MS^n analyses were performed using a ThermoFinnigan LCQ Deca XP Max ion-trap mass spectrometer equipped with Xcalibur software. Column chromatography was performed over Sephadex LH-20 (Pharmacia). Silica Gel 60 (0.040−0.063 mm; Carlo Erba) was used as column material. Semipreparative RP-HPLC separations were conducted on a Waters 590 system equipped with a Waters R401 refractive index detector and with a Waters μ-Bondapak C_{18} column (300 mm × 7.7 mm i.d.,Waters, Milford, MA). TLC was performed on precoated Kieselgel 60 F_{254} plates (Merck, Darmstadt, Germany); compounds were detected by $Ce(SO_4)_2/H_2SO_4$ (Sigma-Aldrich, Milano, Italy) solution, and reagent grade chemicals (Carlo Erba) were used throughout.

Compounds purity was verified by HPLC/UV/MS analyses, and it resulted in ≥95% for all the 24 identified compounds.

3.2. Plant Material. The aerial parts of *Salvia dominica* L. were collected in April 2005 at As-Subayhhi, in Al-Balqa Provine, Jordan, and identified by Dr. Ammar Bader. A voucher specimen number has been deposited in the Herbarium of Laboratory of Pharmacognosy and Phytochemistry at Al-Zaytoonah Private University of Jordan.

3.3. Extraction and Isolation. The dried aerial parts of *S. dominica* (180 g) were powdered and exhaustively extracted using hexane (3.8 g), chloroform (7.2 g), chloroform−methanol (3.5 g), and methanol (6 g), by ASE 2000.

Part of $CHCl_3$−MeOH residue (3.0 g) was submitted to chromatographic separation on a Sephadex LH-20 column using MeOH as mobile phase; fractions were collected, analyzed by TLC on silica 60 F_{254} gel-coated glass sheets with $CHCl_3$−MeOH-H_2O (40:9:1) and $CHCl_3$−MeOH (9:1) and grouped to obtain eight fractions (1−8). The obtained fractions were purified by preliminary SPE followed by RP-HPLC with MeOH−H_2O as mobile phase. (Details are reported in Supporting Information).

Compound 1. Colorless amorphous powder; $[\alpha]_D^{25}$+ 67 (c = 0.1 MeOH). UV (MeOH) λ_{max} (log ε) 272 (9.0). HRMS (positive ion): found m/z 407.256 $[M + Na]^+$; calculated for $C_{25}H_{36}O_3$ 384.266. ESIMS m/z 407 $[M + Na]^+$, 389 $[M + Na\text{-}18]^+$, 371 $[M + H\text{-}36]^+$. ^{1}H and ^{13}C NMR data: Table 1.

Compound 2. Colorless amorphous powder; $[\alpha]_D^{25}$+ 44 (c = 0.1 MeOH). UV (MeOH) λ_{max} (log ε) 332 (9.5). HRMS (positive ion): found m/z 441.264 $[M + Na]^+$; calculated for $C_{25}H_{38}O_5$ 418.272. ESIMS m/z 441 $[M + Na]^+$, 423 $[M + Na\text{-}18]^+$, 405 $[M + Na\text{-}36]^+$. ^{1}H and ^{13}C NMR data: Table 1.

Compound 3. Colorless amorphous powder; $[\alpha]_D^{25}$+ 37 (c = 0.1 MeOH). UV (MeOH) λ_{max} (log ε) 332 (9.5). HRMS (positive ion): found m/z 455.249 $[M + Na]^+$; calculated for $C_{25}H_{36}O_6$ 432.251. ESIMS m/z 455 $[M + Na]^+$, 437 $[M + Na\text{-}18]^+$, 419 $[M + Na\text{-}36]^+$. ^{1}H and ^{13}C NMR data: Table 2.

Compound 4. Colorless amorphous powder; $[\alpha]_D^{25}$+ 72 (c = 0.1 MeOH). UV (MeOH) λ_{max} (log ε) 332 (9.5). HRMS (positive ion): found m/z 457.266 $[M + Na]^+$; calculated for $C_{25}H_{38}O_6$ 434.267. ESIMS m/z 457 $[M + Na]^+$, 439 $[M + Na\text{-}18]^+$, 421 $[M + Na\text{-}36]^+$, 403 $[M + Na\text{-}54]^+$. ^{1}H and ^{13}C NMR data: Table 2.

Compound 5. Colorless amorphous powder; $[\alpha]_D^{25}$+ 69 (c = 0.1 MeOH). UV (MeOH) λ_{max} (log ε) 332 (9.5). HRMS (positive ion): found m/z 485.293 $[M + Na]^+$; calculated for $C_{27}H_{42}O_6$ 462.298. ESIMS m/z 485 $[M + H]^+$, 467 $[M + Na\text{-}18]^+$, 449 $[M + Na\text{-}36]^+$. ^{1}H NMR data (CD_3OD, 600 MHz) δ 0.90 (3H, s, Me-25), 1.07 (3H, s, Me-24), 1.19 (3H, s, Me-22), 1.20 (1H, dd, J = 6.0, 5.0 Hz, H-9), 1.21 (3H, m, $\underline{CH_3}CH_2O$), 1.52 (1H, dd, J = 13.0, 12.0 Hz, H-7b), 1.59 (1H, d, J = 10.0 Hz, H-5), 1.71 (3H, br s, Me-21), 2.15 (1H, ddd, J = 13.5, 6.0, 3.3 Hz, H-12b), 2.22 (3H, d, J = 1.2 Hz, Me-20), 2.30 (1H, dd, J = 12.0, 4.8 Hz, H-7a), 2.34 (1H, ddd, J = 13.5, 11.0, 3.5 Hz, H-12a), 3.44 (1H, m, $CH_3\underline{CH_2}O$), 3.77 (1H, m, $CH_3\underline{CH_2}O$), 3.79 (1H, ddd, J = 11.0, 10.0, 4.8 Hz, H-6), 4.58 (1H, s, H-23), 4.78 (1H, dd, J = 9.2, 2.5 Hz, H-15), 4.99 (1H, d, J = 2.5 Hz, H-16), 5.28 (1H, d, J = 9.2 Hz, H-14), 5.96 (1H, d, J = 1.2, Hz, H-18). ^{13}C NMR data: Table 2.

Compound 6. Colorless amorphous powder; $[\alpha]_D^{25}$+ 109 (c = 0.1 MeOH). UV (MeOH) λ_{max} (log ε) 274 (9.8). HRMS (positive ion): found m/z 469.318 $[M + Na]^+$; calculated for $C_{27}H_{42}O_5$ 446.303. ESIMS m/z 469 $[M + Na]^+$, 451 $[M + Na\text{-}18]^+$. ^{1}H NMR data (CD_3OD, 600 MHz) δ 0.89 (3H, s, Me-25), 1.06 (3H, s, Me-24), 1.18 (3H, s, Me-22), 1.20 (3H, m, $\underline{CH_3}CH_2O$), 1.22 (1H, dd, J = 6.0, 5.0 Hz, H-9), 1.57 (1H, d, J = 10.0 Hz, H-5), 1.70 (3H, br s, Me-21), 2.04 (1H, ddd, J = 13.5, 6.0, 3.3 Hz, H-12b), 2.14 (1H, ddd, J = 13.5, 11.0, 3.5 Hz, H-12a), 2.20 (3H, d, J = 1.2 Hz, Me-20), 2.21 (1H, dd, J = 12.0, 4.8 Hz, H-7a), 2.40 (1H, dd, J = 13.6, 6.0, 3.0 Hz, H-15a), 2.74 (1H, dd, J = 13.6, 8.0, 6.0 Hz, H-15b), 3.40 (1H, m, $CH_3\underline{CH_2}O$), 3.79 (1H, m, $CH_3\underline{CH_2}O$), 3.77 (1H, ddd, J = 12.0, 10.0, 4.8 Hz, H-6), 4.59 (1H, d, J = 8.7 Hz, H-23), 5.07 (1H, m, H-16), 5.09 (1H, dd, J = 8.2, 3.0 Hz, H-14), 5.87 (1H, d, J = 1.2 Hz, H-18). ^{13}C NMR data: Table 2.

Compound 7. Colorless amorphous powder; $[\alpha]_D^{25}$+ 46 (c = 0.1 MeOH). UV (MeOH) λ_{max} (log ε) 332 (9.5). HRMS (positive ion): found m/z 459.286 $[M + Na]^+$; calculated for $C_{25}H_{40}O_6$ 436.283. ESIMS m/z 459 $[M + Na]^+$, 441 $[M + Na\text{-}18]^+$, 423 $[M + Na\text{-}36]^+$, 405 $[M + Na\text{-}54]^+$, 387 $[M + Na\text{-}72]^+$. ^{1}H and ^{13}C NMR data: Table 3.

Compound 8. Colorless amorphous powder; $[\alpha]_D^{25}$+ 104 (c 0.05 MeOH); UV (MeOH) λ_{max} (log ε) 274 (9.1). HRMS (positive ion): found m/z 443.291 $[M + Na]^+$; calculated for $C_{25}H_{40}O_5$ 420.288. ESIMS m/z 443 $[M + Na]^+$, 425$[M + Na\text{-}18]^+$, 407 $[M + Na\text{-}36]^+$, 385 $[M + Na\text{-}58]^+$. ^{1}H and ^{13}C NMR data: Table 3.

Compound 9. Colorless amorphous powder; $[\alpha]_D^{25}$ +90 (c = 0.1 MeOH). UV (MeOH) λ_{max} (log ε) 332 (9.5). HRMS (positive ion): found m/z 443.286 $[M + Na]^+$; calculated for $C_{25}H_{40}O_5$ 420.288. ESIMS m/z 443 $[M + Na]^+$, 425 $[M + Na\text{-}18]^+$, 407 $[M + Na\text{-}36]^+$, 385 $[M + Na\text{-}58]^+$. ^{1}H NMR data (CD_3OD, 600 MHz) δ 1.18 (3H, s, Me-23), 0.95 (3H, s, Me-25), 0.99 (1H, d, J = 10.0 Hz, H-5), 1.03 (3H, s, Me-24), 1.15 (3H, s, Me-22), 1.21 (1H, dd, J = 6.5, 5.0 Hz, H-9), 1.60 (1H, dd, J = 14.0, 12.0 Hz, H-7b), 1.79 (3H, br s, Me-21), 2.11 (1H, ddd, J = 13.5, 6.0, 3.3 Hz, H-12b), 2.15 (1H, dd, J = 14.0, 4.8 Hz, H-7a), 2.21 (3H, d, J = 1.3 Hz, Me-20), 2.25 (1H, ddd, J = 13.5, 11.0, 3.5 Hz, H-12a), 3.82 (1H, ddd, J = 11.0, 12.0, 4.8 Hz, H-6), 4.80 (1H, dd, J = 8.7, 3.0 Hz, H-15), 5.00 (1H, d, J = 3.0 Hz, H-16), 5.30 (1H, d, J = 8.7 Hz, H-14), 5.95 (1H, d, J = 1.3, Hz, H-18). ^{13}C NMR data: Table 3.

Compound 10. Colorless amorphous powder; $[\alpha]_D^{25}$+ 47 (c = 0.1 MeOH). UV (MeOH) λ_{max} (log ε) 332 (9.5). HRMS (positive ion):found m/z 473.259 $[M + Na]^+$; calculated for $C_{25}H_{38}O_7$ 450.261. ESIMS m/z 473 $[M + Na]^+$, 455 $[M + Na\text{-}18]^+$, 437 $[M + Na\text{-}36]^+$. ^{1}H NMR data (CD_3OD, 600 MHz) δ 0.90 (3H, s, Me-25), 1.21 (3H, s, Me-22), 1.25 (3H, s, Me-24), 1.59 (1H, dd, J = 12.0, 13.0 Hz, H-7b), 1.79 (3H, br s, Me-21), 2.05 (1H, d, J = 10.0 Hz, H-5), 2.08 (1H, ddd, J = 13.5, 6.5, 3.8 Hz, H-12b), 2.14 (1H, dd, J = 13.0, 4.8 Hz, H-7a), 2.20 (3H, d, J = 1.3 Hz, Me-20), 2.25 (1H, ddd, J = 13.5, 11.0, 3.8 Hz, H-12a), 3.81 (1H, ddd, J = 11.0, 10.0, 4.8 Hz, H-6), 4.80 (1H, dd, J = 8.5, 3.0 Hz, H-15), 4.98 (1H, d, J = 3.0 Hz, H-16), 5.29 (1H, d, J = 8.5 Hz, H-14), 5.95 (1H, d, J = 1.3, Hz, H-18). ^{13}C NMR data: Table 3.

Compound 11. Colorless amorphous powder; $[\alpha]_D^{25}$+ 58 (c = 0.1 MeOH). UV (MeOH) λ_{max} (log ε) 274 (9.1). HRMS (positive ion): found m/z 457.263 $[M + Na]^+$; calculated for $C_{25}H_{38}O_6$ 434.267. ESIMS m/z 457 $[M + Na]^+$, 439 $[M + Na\text{-}18]^+$, 421 $[M + Na\text{-}36]^+$. ^{1}H NMR data (CD_3OD, 600 MHz) δ 0.91 (3H, s, Me-25), 1.19 (3H, s, Me-22), 1.23 (3H, s, Me-24), 1.61 (1H, dd, J = 11.0, 13.5 Hz, H-7b), 1.70 (3H, br s, Me-21), 2.01 (1H, ddd, J = 13.5, 6.5, 3.8 Hz, H-12b), 2.03 (1H, d, J = 10.5 Hz, H-5), 2.13 (1H, dd, J = 13.5, 4.0 Hz, H-7a), 2.15 (1H, ddd, J = 13.0, 10.5, 4.0 Hz, H-12a), 2.22 (3H, d, J = 1.2 Hz, Me-20), 2.38 (1H, dd, J = 14.0, 5.5, 3.0 Hz, H-15b), 2.68 (1H, dd, J = 14.0, 8.0, 5.5 Hz, H-15a), 4.01 (1H, ddd, J = 11.0, 10.5, 4.0 Hz, H-6), 5.08 (1H, m, H-16), 5.05 (1H, dd, J = 8.0, 3.0 Hz, H-14), 5.88 (1H, d, J = 1.2, Hz, H-18). ^{13}C NMR data: Table 3.

Compound 12. Colorless amorphous powder; $[\alpha]_D^{25}$+ 50 (c = 0.1 MeOH). UV (MeOH) λ_{max} (log ε) 332 (9.5).HRMS (positive ion): found m/z 487.270 [M + Na]$^+$; calculated for $C_{26}H_{40}O_7$ 464.277. ESIMS m/z 487 [M + Na]$^+$, 469 [M + Na-18]$^+$, 389 [M + Na-98]$^+$, 371 [M + Na-116]$^+$. ^{1}H NMR data (CD_3OD, 600 MHz) δ 0.93 (3H, s, Me-25), 1.20 (3H, s, Me-22), 1.28 (3H, s, Me-24), 1.64 (1H, dd, J = 13.0, 4.0 Hz, H-7b), 1.82 (3H, br s, Me-21), 2.09 (1H, d, J = 11.0 Hz, H-5), 2.12 (1H, dd, J = 13.0, 12.0 Hz, H-7a), 2.14 (1H, ddd, J = 13.5, 6.5, 3.8 Hz, H-12b), 2.20 (3H, d, J = 1.2 Hz, Me-20), 2.30 (1H, ddd, J = 13.5, 11.0, 3.8 Hz, H-12a), 3.65 (3H, s, −OMe), 3.69 (1H, ddd, J = 11.0, 12.0, 4.0 Hz, H-6), 4.75 (1H, dd, J = 8.7, 2.0 Hz, H-15), 4.96 (1H, d, J = 2.0 Hz, H-16), 5.29 (1H, d, J = 8.7 Hz, H-14), 5.95 (1H, d, J = 1.2, Hz, H-18). ^{13}C NMR data: Table 3.

Compound 13. Colorless amorphous powder; $[\alpha]_D^{25}$+ 55 (c = 0.1 MeOH). UV (MeOH) λ_{max} (log ε) 332 (9.5). HRMS (positive ion): found m/z 457.265 [M + Na]$^+$; calculated for $C_{25}H_{38}O_6$ 434.267. ESIMS m/z 457 [M + Na]$^+$, 439 [M + Na-18]$^+$, 421 [M + Na-36]$^+$, 403 [M + Na-54]$^+$. ^{1}H and ^{13}C NMR data: Table 4.

Compound 14. Colorless amorphous powder; $[\alpha]_D^{25}$+ 95 (c = 0.1 MeOH). UV (MeOH) λ_{max} (log ε) 274 (9.1). HRMS (positive ion): found m/z 441.268 [M + Na]$^+$; calculated for $C_{25}H_{38}O_5$ 418.272. ESIMS m/z 441 [M + Na]$^+$, 423 [M + Na-18]$^+$, 405 [M + Na-36]$^+$. ^{1}H NMR data (CD_3OD, 600 MHz) δ 0.93 (3H, s, Me-25), 1.18 (3H, s, Me-24), 1.19 (3H, s, Me-22), 1.59 (1H, dd, J = 12.0, 13.0 Hz, H-7b), 1.61 (1H, d, J = 10.0 Hz, H-5), 1.71 (3H, br s, Me-21), 2.02 (1H, ddd, J = 13.5, 6.5, 3.8 Hz, H-12b), 2.14 (1H, dd, J = 12.0, 4.5 Hz, H-7a), 2.15 (3H, d, J = 1.2 Hz, Me-20), 2.17 (1H, ddd, J = 13.5, 11.0, 3.8 Hz, H-12a), 2.41 (1H, dd, J = 14.0, 6.0, 3.5 Hz, H-15b), 2.75 (1H, dd, J = 14.0, 8.0, 5.5 Hz, H-15a), 3.66 (1H, ddd, J = 12.0, 10.0, 4.5 Hz, H-6), 5.08 (1H, dd, J = 8.0, 3.0 Hz, H-16), 5.06 (1H, m, H-14), 5.87 (1H, d, J = 1.2, Hz, H-18), 9.30 (1H, s, H-23), ^{13}C NMR data: Table 4.

Compound 15. Colorless amorphous powder; $[\alpha]_D^{25}$+ 45 (c = 0.1 MeOH). UV (MeOH) λ_{max} (log ε) 332 (9.5). HRMS (positive ion): found m/z 441.270 [M + Na]$^+$; calculated for $C_{25}H_{38}O_5$ 418.272. ESIMS m/z 441 [M + Na]$^+$, 423 [M + Na-18]$^+$, 405 [M + Na-36]$^+$, 387 [M + Na-54]$^+$. ^{1}H and ^{13}C NMR data: Table 4.

Compound 16. Colorless amorphous powder; $[\alpha]_D^{25}$+ 16 (c = 0.1 MeOH). UV (MeOH) λ_{max} (log ε) 332 (9.5). HRMS (positive ion): found m/z 439.251 [M + Na]$^+$; calculated for $C_{25}H_{36}O_5$ 416.256. ESIMS m/z 439 [M + Na]$^+$, 421 [M + Na-18]$^+$, 403 [M + H-36]$^+$. ^{1}H NMR data (CD_3OD, 600 MHz) δ 0.89 (3H, s, Me-25), 1.19 (3H, s, Me-24), 1.38 (1H, d, J = 10.5 Hz, H-5), 1.81 (3H, br s, Me-21), 2.00 (1H, br t, J = 12.0 Hz, H-7b), 2.16 (1H, ddd, J = 13.5, 6.5, 3.8 Hz, H-12b), 2.19 (3H, d, J = 1.2 Hz, Me-20), 2.30 (1H, ddd, J = 13.5, 11.0, 3.8 Hz, H-12a), 2.59 (1H, dd, J = 12.4, 4.9 Hz, H-7a), 3.80 (1H, ddd, J = 12.0, 10.5, 4.9 Hz, H-6), 4.80 (1H, dd, J = 8.7, 2.5 Hz, H-15), 4.98 (1H, d, J = 2.5 Hz, H-16), 5.31 (1H, d, J = 8.7 Hz, H-14), 5.92 (1H, d, J = 1.2, Hz, H-18), 9.38 (1H, s, H-23). ^{13}C NMR data: Table 4.

Compound 17. Colorless amorphous powder; $[\alpha]_D^{25}$+ 20 (c = 0.1 MeOH). UV (MeOH) λ_{max} (log ε) 350 (9.7). HRMS (positive ion): found m/z 441.269 [M + Na]$^+$; calculated for $C_{25}H_{38}O_5$ 418.272. ESIMS m/z 441 [M + Na]$^+$, 423 [M + Na-18]$^+$, 405 [M + Na-36]$^+$. ^{1}H and ^{13}C NMR data: Table 5.

Compound 18. Colorless amorphous powder; $[\alpha]_D^{25}$+ 23 (c = 0.1 MeOH). UV (MeOH) λ_{max} (log ε) 350 (9.7). HRMS (positive ion): found m/z 455.249 [M + Na]$^+$; calculated for $C_{25}H_{36}O_6$ 432.251. ESIMS m/z 455 [M + Na]$^+$, 437 [M + Na-18]$^+$, 419 [M + Na-36]$^+$. ^{1}H NMR data (CD_3OD, 600 MHz) δ 0.91 (3H, s, Me-25), 1.20 (3H, s, Me-22), 1.25 (3H, s, Me-24), 1.64 (1H, dd, J = 12.0, 13.0 Hz, H-7b), 1.98 (3H, d, J = 1.1 Me-21), 2.08 (1H, d, J = 11.0 Hz, H-5), 2.14 (1H, dd, J = 13.5, 4.8 Hz, H-7a), 2.27 (3H, d, J = 1.2 Hz, Me-20), 2.30 (1H, ddd, J = 12.5, 5.5, 4.0 Hz, H-12b), 2.51 (1H, ddd, J = 12.5, 11.5, 4.0 Hz, H-12a), 3.70 (1H, ddd, J = 11.0, 12.0, 4.8 Hz, H-6), 6.01 (1H, d, J = 1.2 Hz, H-18). 6.28 (1H, d, J = 11.8, Hz, H-15), 6.40 (1H, dd, J = 11.8, 1.1 Hz, H-14). ^{13}C NMR data: Table 5.

Compound 19. Colorless amorphous powder; $[\alpha]_D^{25}$+ 30 (c = 0.1 MeOH). UV (MeOH) λ_{max} (log ε) 350 (9.7). HRMS (positive ion): found m/z 439.253 [M + Na]$^+$; calculated for $C_{25}H_{36}O_5$ 416.256. ESIMS m/z 439 [M + Na]$^+$, 421 [M + Na-18]$^+$, 403 [M + H-36]$^+$. ^{1}H NMR data (CD_3OD, 600 MHz) δ 0.94 (3H, s, Me-25), 1.18 (3H, s, Me-24), 1.21 (3H, s, Me-22), 1.58 (1H, dd, J = 12.5, 13.0 Hz, H-7b), 1.61 (1H, d, J = 10.0 Hz, H-5), 1.98 (3H, d, J = 1.1 Me-21), 2.13 (1H, dd, J = 13.0, 3.5 Hz, H-7a), 2.25 (3H, d, J = 1.3 Hz, Me-20), 2.28 (1H, ddd, J = 14.5, 6.5, 4.5 Hz, H-12b), 2.44 (1H, ddd, J = 14.5, 12.0, 4.2 Hz, H-12a), 3.63 (1H, ddd, J = 12.0, 10.0, 3.0 Hz, H-6), 6.00 (1H, d, J = 1.3 Hz, H-18), 6.30 (1H, d, J = 11.6, Hz, H-15), 6.41 (1H, dd, J = 11.6, 1.1 Hz, H-14), 9.52 (1H, s, H-25). ^{13}C NMR data: Table 5.

Compound 20. Colorless amorphous powder; $[\alpha]_D^{25}$+ 33 (c = 0.1 MeOH). UV (MeOH) λ_{max} (log ε) 350 (9.7). HRMS (positive ion): found m/z 437.235 [M + Na]$^+$; calculated for $C_{25}H_{34}O_5$ 414.241. ESIMS m/z 437 [M + Na]$^+$, 419 [M + Na-18]$^+$. ^{1}H NMR data (CD_3OD, 600 MHz) δ 0.99 (3H, s, Me-25), 1.23 (3H, s, Me-22), 1.24 (3H, s, Me-24), 1.58 (1H, d, J = 10.0 Hz, H-5), 1.65 (1H, dd, J = 12.0, 13.0 Hz, H-7b), 1.98 (3H, d, J = 1.1 Me-21), 2.16 (1H, dd, J = 12.0, 3.5 Hz, H-7a), 2.32 (1H, ddd, J = 13.5, 6.5, 3.8 Hz, H-12b), 2.25 (3H, d, J = 1.2 Hz, Me-20), 2.51 (1H, ddd, J = 13.5, 11.0, 3.8 Hz, H-12a), 4.43 (1H, ddd, J = 12.0, 10.0, 3.5 Hz, H-6), 5.99 (1H, d, J = 1.2 Hz, H-18), 6.29 (1H, d, J = 11.8, Hz, H-15), 6.41 (1H, dd, J = 11.8, 1.2 Hz, H-14). ^{13}C NMR data: Table 5.

Compound 21. Colorless amorphous powder; $[\alpha]_D^{25}$+ 32 (c = 0.1 MeOH); UV (MeOH) λ_{max} (log ε) 350 (9.7). HRMS (positive ion): found m/z 439.259 [M + Na]$^+$; calculated for $C_{25}H_{36}O_5$ 416.256. ESIMS m/z 439 [M + H]$^+$, 421 [M + Na-18]$^+$. ^{1}H and ^{13}C NMR data: Table 5.

Compound 22. Colorless amorphous powder; $[\alpha]_D^{25}$+ 54 (c = 0.1 MeOH). UV (MeOH) λ_{max} (log ε) 277 (8.9). HRMS (positive ion): found m/z 475.271 [M + Na]$^+$; calculated for $C_{25}H_{40}O_7$ 452.277. ESIMS m/z 475 [M + Na]$^+$, 457 [M + Na-18]$^+$, 439 [M + Na-36]$^+$, 421 [M + H-54]$^+$, 403 [M + H-72]$^+$. ^{1}H and ^{13}C NMR data: Table 6.

Compound 23. Colorless amorphous powder; $[\alpha]_D^{25}$+ 13 (c = 0.1 MeOH). UV (MeOH) λ_{max} (log ε) 277 (8.9). HRMS (positive ion): found m/z 475.274 [M + Na]$^+$; calculated for $C_{25}H_{40}O_7$ 452.277. ESIMS m/z 475 [M + Na]$^+$, 457 [M + Na-18]$^+$, 439 [M + Na-36]$^+$, 421 [M + H-54]$^+$, 403 [M + H-72]$^+$. ^{1}H and ^{13}C NMR data: Table 6.

Compound 24. Colorless amorphous powder; $[\alpha]_D^{25}$+ 38 (c = 0.1 MeOH). UV (MeOH) λ_{max} (log ε) 277 (8.9). HRMS (positive ion): found m/z 473.260 [M + Na]$^+$; calculated for $C_{25}H_{38}O_7$ 450.262. ESIMS m/z 473 [M + Na]$^+$, 455 [M + Na-18]$^+$, 437 [M + Na-36]$^+$, 419 [M + H-54]$^+$. ^{1}H NMR data (CD_3OD, 600 MHz) δ 0.93 (3H, s, Me-25), 1.19 (3H, s, Me-24), 1.21 (3H, s, Me-22), 1.55 (1H, dd, J = 12.0, 13.0 Hz, H-7b), 1.62 (1H, d, J = 10.0 Hz, H-5), 2.12 (1H, dd, J = 12.0, 4.8 Hz, H-7a), 2.16 (3H, d, J = 1.2 Hz, Me-20), 2.18 (1H, ddd, J = 14.5, 6.5, 4.5 Hz, H-12b), 2.30 (1H, ddd, J = 14.5, 12.0, 4.2 Hz, H-12a), 3.64 (1H, ddd, J = 11.0, 10.0, 4.0 Hz, H-6), 3.85 (1H, dd, J = 9.0, 1.2, Hz, H-15), 4.21 (1H, d, J = 9.0 Hz, H-14), 5.06 (1H, br s, H-21b), 5.14 (1H, br s, H-21a), 5.38 (1H, d, J = 1.2 Hz, H-16), 5.91 (1H, d, J = 1.2 Hz, H-18), 9.5 (1H, s, H-25). ^{13}C NMR data: Table 6.

Methylation of Compound 1. A solution of compound **1** (25 mg) in benzene (5 mL) was treated with methyl lithium (1.6 M in diethyl ether, 0.1 mL), and the whole was stirred at 0 °C for 30 min under N_2 atmosphere. The reaction mixture was poured into ice−water, and the whole was extracted with AcOEt. The crude product obtained after evaporation of the organic layer was purified by silica gel TLC with $CHCl_3$/MeOH (9:1) as mobile phase to give modified compound **1** (**1a**) (18 mg).

Preparation of MTPA Esters. MTPA esters of compound **1a** were prepared by mixing 4.5 mg of compounds **1a**, (*S*)-(−)-MTPA and (*R*)-(+)-MTPA (17 mg), dicyclohexyl carbodiimide (17 mg), and 4-dimethylaminopyridine (6 mg) in methylene chloride (10 mL) and stirring overnight at room temperature. The dicyclohexylurea that precipitated was removed by filtration. The filtrate was washed successively with 50 mL portions of 0.5 N HCl, 2 N Na_2CO_3, and brine. The crude product obtained

after evaporation of the organic layer was purified by silica gel TLC with $CHCl_3$/MeOH (9:1) as the mobile phase, to give MTPA esters.

Hydrogenation of Compound 2. Compound **2** (64 mg) was hydrogenated at atmospheric pressure over 10% Pd/C in 2 mL of EtOH for 48 h. Removal of the catalyst by filtration and evaporation of the solvent gave mixture of saturated derivatives. After separation of the mixture by preparative TLC with $CHCl_3$−MeOH, the most abudant of the derivatives was selected for acylation using (*S*)-(−)-MTPA and (*R*)-(+)-MTPA (separately). (*S*)-(−)-MTPA and (*R*)-(+)-MTPA esters were preparated under the same conditions as described for compound **1**.

Alkaline Hydrolysis. A solution of hydrogenated compound **2** (50 mg) in 10 mL of MeOH-H_20 (1:1) containing 250 mg of KOH was heated with stirring at 60 °C for 1 h. The reaction mixture was cooled, and the organic solvent was removed in vacuo. The H_2O suspension was acidified with 0.5 N HCl and then extracted with Et_2O (3 × 5 mL). The Et_2O extract was dried over Na_2SO_4. CH_2N_2 (2 mL in Et_2O) was added dropwise to the Et_2O solution at 0 °C. After 15 min at 0 °C, the reaction mixture was quenched with MeOH; the solvent was removed under reduced pressure, and the obtained derivative (10 mg) was purified by chromatography on Si gel.

Preparation of Acetonide Derivatives. Suspensions of compounds **22**, **23**, **24**, and hydrolyzed compound **2** (2.0 mg) in THF (2.0 mL) were separately treated with 2,2-dimethoxypropane (0.5 mL), followed by a catalytic amount of anhydrous *p*-TsOH at 25 °C. After 1 h of stirring, a few drops of Et_3N were added and the mixture was concentrated in vacuo. The residue was partitioned between $CHCl_3$ and a saturated solution of $NaHCO_3$, and the chloroform part was concentrated in vacuo, affording the corresponding acetonides. ^{1}H NMR spectra of the acetonides were recorded.

Chemical Proteomics. Compound **13** was immobilized on alkylamine controlled pore glass beads (0.5 μm) (Millipore, Billerica, MA) by directly incubating 15 μmol of the sesterterpene with 1 g of anhydrous beads in 5 mL of CH_3CN. Under these conditions, the Schiff base formation between the aldehydic group of **13** and the ammine function of the beads was quite efficient, as verified by HPLC analysis of the reaction mixture. After 2 h of incubation, 5 mL of 150 mM $NaBH_4$ in PBS was added to obtain a stable amine. The reaction carried on for 30 min, after which the beads were washed out with water and CH_3CN to remove the unreacted sesterterpene. The modified beads stored in CH_3CN at 4 °C. The same amount of alkylamine controlled pore glass beads was subjected to the same treatment but without compound **13** to prepare a control column.

MCF-7 (breast-cancer) cells were cultured in DMEM medium (Sigma, St. Louis, MO) supplemented with 10% (v/v) fetal bovine serum (Sigma, St. Louis, MO), 100 U/mL penicillin, and 100 μg/mL streptomycin (Sigma, St. Louis, MO) at 37 °C in a 5% CO_2 atmosphere. For protein extracts, cells were harvested and washed three times with PBS 1X (Sigma, St. Louis, MO), cell pellets were resuspended in lysis buffer (20 mM sodium phosphate pH 7.4, 150 mM NaCl, 1% Nonidet P-40) supplemented with protease inhibitor cocktail (Sigma, St. Louis, MO), incubated for 30 min on ice and clarified by centrifugation for 15 min at 12000*g* at 4 °C.

Unloaded and **13**-loaded beads (100 μL) were washed extensively with lysis buffer and then incubated with 1 mg of MCF-7 protein extract for 16 h at 4 °C with continuous shaking on a rotator tube holder. The modified and unmodified beads were washed five times with 10 mL of 20 mM sodium phosphate pH 7.4, 150 mM NaCl, and then eluted with 100 μL of Laemmli sample buffer (2% SDS, 10% glycerol, 1% 2-mercaptoethanol, 0.002% bromphenol blue, 62.5 mM Tris HCl). Eluted samples were loaded on a monodimensional 10% SDS-PAGE, and separated proteins were stained with Brilliant Blue G-Colloidal (Sigma, St. Louis, MO).

Elution of proteins from acrylamide gels and trypsin digestion were performed as described.[49] Briefly, Coomassie-stained protein bands were excised from the polyacrylamide gel, reduced, alkylated using iodoacetamide, and digested by trypsin. The resulting fragments were extracted and analyzed by LC/MS/MS: peptide separation was performed on a capillary BEH C_{18} column (0.075 mm × 100 mm, 1.7 μm Waters) using aqueous 0.1% formic acid (A) and CH_3CN containing 0.1% formic acid (B) as mobile phases. Peptides were eluted by means of linear gradient from 5% to 50% of B in 45 min and a 300 nL/min flow rate. Capillary ion source voltage was set at 2.5 kV, cone voltage at 35 V, and extractor voltage at 3 V. Peptide fragmentation was achieved using argon as collision gas and a collision cell energy of 25 eV. Mass spectra were acquired in a *m*/*z* range from 400 to 1800, and MS/MS spectra in a 25−2000 range. Mass and MS/MS spectra calibration was performed using a mixture of angiotensin and insulin as external standard and [Glu]-Fibrinopeptide B human as lock mass standard.

MS and MS/MS data were used by Mascot Version 2.1.03 (Matrix Science) and Protein Prospector 5.1.8 basic (UCSF) to interrogate the National Center for Biotechnology Information nonredundant (NCBInr) protein database. Settings were as follows: mass accuracy window for parent ion, 50 ppm; mass accuracy window for fragment ions, 200 millimass units; fixed modification, carbamidomethylation of cysteines; variable modifications, oxidation of methionine.

Surface Plasmon Resonance Analyses. SPR analyses were performed on a Biacore 3000 optical biosensor equipped with research-grade CM5 sensor chips (Biacore AB). Using this platform, two separate TTL (Tebu-Bio, Milan, Italy) surfaces, one BSA surface and one unmodified reference surface, were prepared for simultaneous analyses. Immediately after chip docking, the instrument was primed with water and the sensor chip surfaces were preconditioned by applying two consecutive 20 μL injections each (at a flow rate of 100 μL/min) of 50 mM NaOH, 10 mM HCl, 0.1% SDS (w/v), and 10 mM H_3PO_4. Prior to each interaction analysis, the biosensor detector response was normalized (automated procedure) and the instrument was primed five times with running buffer (10 mM NaH_2PO_4, 150 mM NaCl, 0.5% DMSO, pH 7.4). Data were collected at 2.5 Hz. Proteins (100 μg/mL in 10 mM sodium acetate, pH 5.0) were immobilized on individual sensor chip surfaces at a flow rate of 5 μL/min using standard amine-coupling protocols[50] to obtain densities of 8−12 kRU.

Compounds **1**−**24** were dissolved in 100% DMSO to obtain 4 mM solutions and diluted 1:200 (v/v) in PBS (10 mM NaH_2PO_4, 150 mM NaCl, pH 7.4) to a final DMSO concentration of 0.5%. Compounds concentration series were prepared as 2-fold dilutions into running buffer: for each sample, the complete binding study was performed using a 5 points concentration series, typically spanning 0.05−10 μM, and triplicate aliquots of each compound concentration were dispensed into single-use vials, capped, and randomized in the instrument's autosampler rack. Included in each analysis were multiple blank samples of running buffer alone. Five of these blanks were analyzed at the beginning of the analysis, and the remaining blanks were interspersed throughout the analysis for double-referencing purposes.[51] Binding experiments were performed at 25 °C, using a flow rate of 50 μL/min, with 60 s monitoring of association and 200 s monitoring of dissociation. Regeneration of the surfaces was performed by a 140 s injection of 50 mM glycine (pH 9.5), followed by an ExtraClean wash command that automatically flushes the sample delivery system with running buffer.

SPR response data (sensorgrams) were zeroed on both the response and time axes at the beginning of each injection and double referenced. First, bulk refractive index changes were corrected by subtracting the responses generated over an unmodified reference surface from the binding responses generated over the albumin and TTL surfaces. Second, any systematic artifacts observed between the TTL and reference flow cells were corrected by subtracting the response generated by an average of the buffer injections from the binding responses generated by compounds injections. Hallmarks that make this data set a good one include responses that are concentration dependent, replicate injections that overlay, and clearly discernible exponential curvature during both the association and dissociation phases.[52] Simple interactions were adequately fit to a single-site bimolecular interaction model (A + B = AB),

yielding a single K_D. Sensorgram elaborations were performed using the Biaevaluation software provided by Biacore AB.

Cytoxicity Assays. MTT assays were performed using MCF-7, J744.A1, HEK293 cell lines. About 5×10^3 viable cells were plated in 96-well plates, after 24 h, compounds **1**−**24** were added at different concentrations (25, 50, 100, and 200 μM) for different times of incubation (24 and 48 h). Then 3-[4, 5-dimethylthiazol-2-yl]-2,5-diphenyl tetrazolium bromide (MTT) dye was added at a final concentration of 0.5 mg/mL, and cells were incubated for 1 h at 37 °C. Insoluble purple formazan christals were solubilized with DMSO, and absorbance was examined at 570 nm with reference at 620 nm by use of a microplate reader.

Western Blot Analysis. MCF-7 cells were seeded in a 6-well plastic plate at 4×10^5 cells per well. After 24 h, cells were incubated with or without 100 μM of compound **11** for 24 and 48 h. At the end of the treatments, cells were harvested and washed three times with PBS 1X, cell pellets were resuspended in lysis buffer (20 mM sodium phosphate pH 7.4, 150 mM NaCl, 1% Nonidet P-40), incubated for 30 min on ice, and clarified by centrifugation for 15 min at 12000*g* at 4 °C. Protein concentration was determined with Bradford method, equal amounts (20 μg) of each sample were separated on a 10% SDS-PAGE and then electroblotted on a Hybond-ECL membrane (GE Heathcare) for 1 h at 4 °C at 100 V. The membrane was saturated with 5% nonfat dry milk (BioRad, Hercules, CA) for 1 h at room temperature and then incubated with rabbit polyclonal antibody anti-Δ2-α-tubulin (Chemicon International, Temecula, CA) overnight at 4 °C. A donkey antirabbit (Jackson) was used as a secondary antibody and ECL system (GE Healthcare) for detection.

Supporting Information Available: Stereochemistry of compounds **1** and **2**, extraction and isolation, LC/MSn analysis of crude acetone extract of *S. dominica*, cytotoxicity of compound **11**. This material is available free of charge via the Internet at http://pubs.acs.org.

References

(1) Foster, S.; Tyler, V. E. *Tyler's Honest Herbal*, 4th ed.; The Haworth Press: Binghamton, NY, 2000; pp 327−329 and 414−415.
(2) Steinegger, E.; Hansel, R. *Lehrbuch der Pharmakognosie*, 4th ed.; Springer-Verlag: Berlin, 1988; pp 343−345.
(3) Bozan, B.; Ozturk, N.; Kosar, M.; Tunalier, Z.; Baser, K. H. C. Antioxidant and free radical scavenging activities of eight *Salvia* species. *Chem. Nat. Compounds* **2002**, *38* (2), 198–200.
(4) Ulubelen, A. In *The genus Salvia. Medicinal and Aromatic Plants-Industrial Profiles*; Kintzios, S. E., Ed.; Harwood Academic Publishers: Amsterdam, 2000; Vol. 14, pp 55−68.
(5) Topcu, G. Bioactive triterpenoids from *Salvia* species. *J. Nat. Prod.* **2006**, *69*, 482–487.
(6) Yang, M. H.; Blunden, G.; Xu, Y. X.; Nagy, G.; Mathe, I. Diterpenoids from *Salvia* species. *Pharm. Sci.* **1996**, *2*, 69–71.
(7) Al-Eisawi, D. M. *Field Guide to Wild Flowers of Jordan and Neighbouring Countries*; The National Library: Amman, 1998.
(8) Feinbrun-Dothan, N. *Flora Palaestina Part III*; The Israel Academy of Science & Humanities: Jerusalem, 1978.
(9) Liu, Y.; Wang, L.; Jung, J. H.; Zhang, S. Sesterterpenoids. *Nat. Prod. Rep.* **2007**, *24*, 1401–1429.
(10) Blunt, J. W.; Copp, B. R.; Hu, W.-P.; Munro, M. H. G.; Northcote, P. T.; Prinsep, M. R. Marine natural products. *Nat. Prod. Rep.* **2007**, *24*, 31–86.
(11) Katayama, H.; Oda, Y. Chemical proteomics for drug discovery based on compound-immobilized affinity chromatography. *J. Chromatogr., B.* **2007**, *855*, 21–27.
(12) Barra, H. S.; Arce, C. A.; Argarana, C. E. Posttranslational tyrosination/detyrosination of tubulin. *Mol. Neurobiol.* **1988**, *2*, 133–153.
(13) Ersfeld, K.; Wehland, J.; Plessmann, U.; Dodemont, H.; Gerke, V.; Weber, K. Characterization of the tubulin−tyrosine ligase. *J. Cell. Biol.* **1993**, *120*, 725–732.
(14) Erck, C.; Peris, L.; Andrieux, A.; Meissirel, C.; Gruber, A. D.; Vernet, M.; Schweitzer, A.; Saoudi, Y.; Pointu, H.; Bosc, C.; Salin, P. A.; Job, D.; Wehland, J. A vital role of tubulin−tyrosine ligase for neuronal organization. *Proc. Nat. Acad. Sci. U.S.A.* **2005**, *102*, 7853–7858.
(15) Mialhe, A.; Lafanechere, L.; Treilleux, I.; Peloux, N.; Dumontet, C.; Bremond, A.; Panh, M. H.; Payan, R.; Wehland, J.; Margolis, R. L.; Job, D. Tubulin detyrosination is a frequent occurrence in breast cancers of poor prognosis. *Cancer Res.* **2001**, *61*, 5024–5027.
(16) Kato, C.; Miyazaki, K.; Nakagawa, A.; Ohira, M.; Nakamura, Y.; Ozaki, T.; Imai, T.; Nakagawara, A. Low expression of human tubulin tyrosine ligase and suppressed tubulin tyrosination/detyrosination cycle are associated with impaired neuronal differentiation in neuroblastomas with poor prognosis. *Int. J. Cancer* **2004**, *112*, 365–75.
(17) Soucek, K.; Kamaid, A.; Phung, A. D.; Kubala, L.; Bulinski, J. C.; Harper, R. W.; Eiserich, J. P. Normal and prostate cancer cells display distinct molecular profiles of α-tubulin posttranslational modifications. *Prostate* **2006**, *66*, 954–965.
(18) Tanaka, R.; Aoki, H.; Wada, S.; Matsunaga, S. Two Novel Lanostane-Type Triterpenes from the Stem Bark of *Abies mariesii*. *J. Nat. Prod.* **1999**, *62*, 198–200.
(19) Rustaiyan, A.; Sadjadi, A. Salvisyriacolide, a sesterterpene from *Salvia syriaca*. *Phytochemistry* **1987**, *26*, 3078–3079.
(20) Charan, R. D.; McKee, T. C.; Boyd, M. R. Thorectandrols C, D, and E, new sesterterpenes from the marine sponge *Thorectandra* sp. *J. Nat. Prod.* **2002**, *65*, 492–495.
(21) Linden, A.; Juch, M.; Moghaddam, F. M.; Zaynizadeh, B.; Rueedi, P. The absolute configuration of salvileucolide methyl ester, a sesterterpene from Iranian *Salvia* species. *Phytochemistry* **1996**, *41*, 589–590.
(22) Kusumi, T.; Ohtani, I.; Inouye, Y.; Kakisawa, H. Absolute configurations of cytotoxic marine cembranolides; consideration of Mosher's method. *Tetrahedron Lett.* **1988**, *29*, 4731–4734.
(23) Ohtani, I.; Kusumi, T.; Kashman, Y.; Kakisawa, H. High-field FT NMR application of Mosher's method. The absolute configurations of marine terpenoids. *J. Am. Chem. Soc.* **1991**, *113*, 4092–4096.
(24) Fontana, A.; Albarella, L.; Scognamiglio, G.; Uriz, M.; Cimino, G. Structural and stereochemical studies of C-21 terpenoids from Mediterranean Spongiidae Sponges. *J. Nat. Prod.* **1996**, *59*, 869–872.
(25) Gu, Z. M.; Fang, X. P.; Zeng, L.; Kozlowski, J. F.; McLaughlin, J. L. Novel cytotoxic annonaceous acetogenins: (2,4-*cis* and *trans*)-bulladecinones from *Annona bullata* (Annonaceae). *Bioorg. Med. Chem. Lett.* **1994**, *4*, 473–478.
(26) Wu, F. E.; Zeng, L.; Gu, Z. M.; Zhao, G. X.; Zhang, Y.; Schwedler, J. T.; McLaughlin, J. L.; Sastrodihardjo, S. New bioactive monotetrahydrofuran annonaceous acetogenins, annomuricin C and muricatocin C, from the leaves of *Annona muricata*. *J. Nat. Prod.* **1995**, *58*, 909–915.
(27) Cioffi, G.; Bader, A.; Malafronte, A.; Dal Piaz, F.; De Tommasi, N. Secondary metabolites from the aerial parts of *Salvia palaestina* Bentham. *Phytochemistry* **2008**, *69*, 1005–1012.
(28) Rustaiyan, A.; Sadjadi, A. Salvisyriacolide, a sesterterpene from *Salvia syriaca*. *Phytochemistry* **1987**, *26*, 3078–3079.
(29) Topcu, G.; Ulubelen, A.; Tam, T. C. M.; Chin, T. C. Sesterterpenes and other constituents of *Salvia yosgadensis*. *Phytochemistry* **1996**, *42*, 1089–1092.
(30) Ngadjui, B. T.; Folefoc, G. G.; Keumedjio, F.; Dongo, E.; Sondengam, B. L.; Connolly, J. D. Crotonadiol, a labdane diterpenoid from the stem bark of *Croton zambesicus*. *Phytochemistry* **1999**, *51*, 171–174.
(31) Tsuda, M.; Shigemori, H.; Ishibashi, M.; Sasaki, T.; Kobayashi, J. Luffariolides A−E, new cytotoxic sesterterpenes from the Okinawan marine sponge *Luffariella* sp. *J. Org. Chem.* **1992**, *57*, 3503–3507.
(32) Moghaddam, F. M.; Zaynizadeh, B.; Rueedi, P. Salvileucolide methyl ester, a sesterterpene from *Salvia sahendica*. *Phytochemistry* **1995**, *39*, 715–716.
(33) Braca, A.; Bader, A.; Siciliano, T.; Morelli, I.; De Tommasi, N. New pyrrolizidine alkaloids and glycosides from *Anchusa strigosa*. *Planta Med.* **2003**, *69*, 835–841.
(34) Katayama, H.; Oda, Y. Chemical proteomics for drug discovery based on compound-immobilized affinity chromatography. *J. Chromatogr., B* **2007**, *855*, 21–27.
(35) Sleno, L.; Emili, A. Proteomic methods for drug target discovery. *Curr. Opin. Chem. Biol.* **2008**, *12*, 46–54.
(36) Kosaka, T.; Okuyama, R.; Sun, W.g.; Ogata, T.; Harada, J.; Araki, K.; Izumi, M.; Yoshida, T.; Okuno, A.; Fujiwara, T.; Ohsumi, J.; Ichikawa, K. Identification of molecular target of amp-activated protein kinase activator by affinity purification and mass spectrometry. *Anal. Chem.* **2005**, *77*, 2050–2055.
(37) Cooper, M. A. Label-free screening of biomolecular interactions. *Anal. Bioanal. Chem.* **2003**, *377*, 834–842.
(38) Westermann, S.; Weber, K. Post-translational modifications regulate microtubule function. *Nat. Rev. Mol. Cell Biol.* **2003**, *4*, 938–947.
(39) Lafanechère, L.; Courtay-Cahen, C.; Kawakami, T.; Jacrot, M.; Rüdiger, M.; Wehland, J.; Job, D.; Margolis, R. L. Suppression of tubulin tyrosine ligase during tumor growth. *J. Cell Sci.* **1998**, *111*, 171–181.
(40) Ueoka, R.; Nakao, Y.; Fujii, S.; van Soest, R. W.; Matsunaga, S. Aplysinoplides A−C, cytotoxic sesterterpenes from the marine sponge *Aplysinopsis digitata*. *J. Nat. Prod.* **2008**, *71*, 1089–1091.
(41) Somerville, M. J.; Hooper, J. N.; Garson, M. J. Mooloolabenes A−E, norsesterterpenes from the Australian sponge *Hyattella intestinalis*. *J. Nat. Prod.* **2006**, *69*, 1587–1590.

(42) Argarana, C. E.; Barra, H. S.; Caputto, R. Release of [^{14}C]tyrosine from tubulinyl-[^{14}C]tyrosine by brain extract: separation of a carboxypeptidase from tubulin−tyrosine ligase. *Mol. Cell. Biochem.* **1978**, *19*, 17–21.
(43) Luduena, R. F. Multiple forms of tubulin: different gene products and covalent modifications. *Int. Rev. Cytol.* **1998**, *178*, 207–275.
(44) Raybin, D.; Flavin, M. Enzyme which specifically adds tyrosine to the alpha chain of tubulin. *Biochemistry* **1977**, *16*, 2189–2194.
(45) Arce, A.; Hallak, M. E.; Rodriguez, J. A.; Barra, H. S.; Caputto, R. Capability of tubulin and microtubules to incorporate and to release tyrosine and phenylalanine and the effect of the incorporation of these amino acids on tubulin assembly. *J. Neurochem.* **1978**, *31*, 205–210.
(46) Badin-Larcon, A. C.; Boscheron, C.; Soleilhac, J. M.; Piel, M.; Mann, C.; Denarier, E.; Fourest-Lieuvin, A.; Lafanechere, L.; Bornens, M.; Job, D. Suppression of nuclear oscillations in *Saccharomyces cerevisiae* expressing Glu-tubulin. *Proc. Natl. Acad. Sci. U.S.A.* **2004**, *101*, 5577–5582.
(47) Vee, S.; Lafanechere, L.; Fisher, D.; Wehland, J.; Job, D.; Picard, A. Evidence for a role of the (alpha)-tubulin C terminus in the regulation of cyclin B synthesis in developing oocytes. *J. Cell Sci.* **2001**, *114*, 887–898.
(48) Eiserich, P.; Estevez, A. G.; Bamberg, T. V.; Ye, Y. Z.; Chumley, P. H.; Beckman, J. S.; Freeman, B. A. Microtubule dysfunction by posttranslational nitrotyrosination of alpha-tubulin: a nitric oxide dependent mechanism of cellular injury. *Proc. Natl. Acad. Sci. U.S.A.* **1999**, *96*, 6365–6370.
(49) Shevchenko, A.; Tomas, H.; Havlis, J.; Olsen, J. V.; Mann, M. In-gel digestion for mass spectrometric characterization of proteins and proteomes. *Nat. Protoc.* **2006**, *1*, 2856–2860.
(50) Johnsson, B.; Loefaas, S.; Lindquist, G. Immobilization of proteins to a carboxymethyldextran-modified gold surface for biospecific interaction analysis in surface plasmon resonance sensors. *Anal. Biochem.* **1991**, *198*, 268–277.
(51) Myszka, D. G. Improving biosensor analysis. *J. Mol. Recogn.* **1999**, *12*, 279–284.
(52) Papalia, G. A.; Leavitt, S.; Bynum, M. A.; Katsamba, P. S.; Wilton, R.; Qiu, H.; Steukers, M.; Wang, S.; Bindu, L.; Phogat, S.; Giannetti, A. M.; Ryan, T. E.; Pudlak, V. A.; Matusiewicz, K.; Michelson, K. M.; Nowakowski, A.; Pham-Baginski, A.; Brooks, J.; Tieman, B. C.; Bruce, B. D.; Vaughn, M.; Baksh, M.; Cho, Y. H.; De Wit, M.; Smets, A.; Vandersmissen, J.; Michiels, L.; Myszka, D. G. Comparative analysis of 10 small molecules binding to carbonic anhydrase II by different investigators using Biacore technology. *Anal. Biochem.* **2006**, *359*, 94–105.

JM801637F